AD-A113 931 COLD REGIONS RESEARCH AND ENGINEERING LAB HANOVER NH F/G 13/9
MECHANICS OF CUTTING AND BORING. PART 7. DYNAMICS AND ENERGETIC--ETC(U)
DEC 81 M MELLOR
UNCLASSIFIED CRREL-81-26 NL

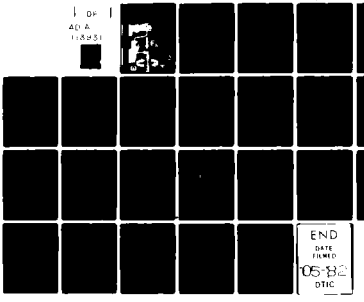

END
DATE FILMED
05-82
DTIC

CRREL

Mechanics of cutting and boring

Part 7: Dynamics and energetics of axial rotation machines

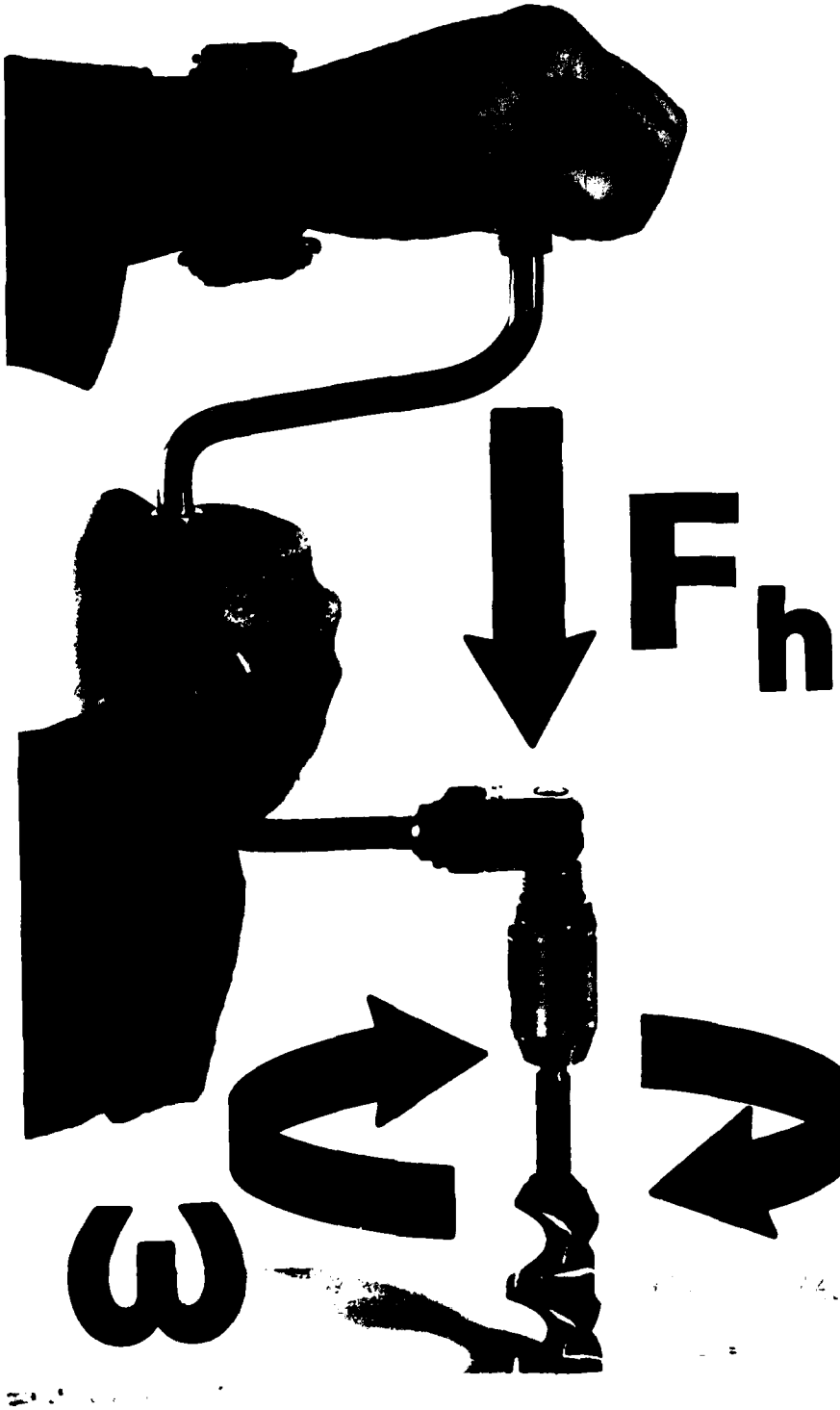

CRREL Report 81-26

Mechanics of cutting and boring

Part 7: Dynamics and energetics of axial rotation machines

Malcolm Mellor

December 1981

Prepared for
OFFICE OF THE CHIEF OF ENGINEERS
By
UNITED STATES ARMY CORPS OF ENGINEERS
COLD REGIONS RESEARCH AND ENGINEERING LABORATORY
HANOVER, NEW HAMPSHIRE, U.S.A.

Unclassified

SECURITY CLASSIFICATION OF THIS PAGE (When Data Entered)

REPORT DOCUMENTATION PAGE	READ INSTRUCTIONS BEFORE COMPLETING FORM
1. REPORT NUMBER: CRREL Report 81-26	2. GOVT ACCESSION NO.: AD-A113 931
3. RECIPIENT'S CATALOG NUMBER	
4. TITLE (and Subtitle): MECHANICS OF CUTTING AND BORING Part 7: Dynamics and Energetics of Axial Rotation Machines	5. TYPE OF REPORT & PERIOD COVERED
	6. PERFORMING ORG. REPORT NUMBER
7. AUTHOR(s): Malcolm Mellor	8. CONTRACT OR GRANT NUMBER(s)
9. PERFORMING ORGANIZATION NAME AND ADDRESS: U.S. Army Cold Regions Research and Engineering Laboratory Hanover, New Hampshire 03755	10. PROGRAM ELEMENT, PROJECT, TASK AREA & WORK UNIT NUMBERS: DA Project 4A762730AT42 Technical Area A, Work Unit 002
11. CONTROLLING OFFICE NAME AND ADDRESS: Office of the Chief of Engineers Washington, D.C. 20314	12. REPORT DATE: December 1981
	13. NUMBER OF PAGES: 46
14. MONITORING AGENCY NAME & ADDRESS (if different from Controlling Office)	15. SECURITY CLASS. (of this report): Unclassified
	15a. DECLASSIFICATION/DOWNGRADING SCHEDULE

16. DISTRIBUTION STATEMENT (of this Report)

Approved for public release; distribution unlimited.

17. DISTRIBUTION STATEMENT (of the abstract entered in Block 20, if different from Report)

18. SUPPLEMENTARY NOTES

19. KEY WORDS (Continue on reverse side if necessary and identify by block number)

Cutting tools	Machines
Drilling	Mechanics
Drilling machines	Permafrost
Drills	Rock drilling
Excavation	

20. ABSTRACT (Continue on reverse side if necessary and identify by block number)

This report deals with force, torque, energy and power in machines such as drills and boring devices, where the cutting head rotates about a central axis while penetrating parallel to that axis. Starting from a consideration of the forces developed on individual cutting tools, or segments of cutters, the thrust and torque on a complete cutting head is assessed, and simple relationships between thrust and torque are derived. Similarly, the energy and power needed to drive the cutting head are estimated and related to tool characteristics. Design characteristics of existing machines are compiled and analyzed to give indications of thrust, torque, power, effective tool forces, nominal thrust pressure, power density, and specific energy.

DD FORM 1 JAN 73 1473 EDITION OF 1 NOV 65 IS OBSOLETE

Unclassified

SECURITY CLASSIFICATION OF THIS PAGE (When Data Entered)

PREFACE

This report was prepared by Dr. Malcolm Mellor, Physical Scientist, Experimental Engineering Division, U.S. Army Cold Regions Research and Engineering Laboratory. This work was funded by DA Project 4A762730AT42, *Design, Construction and Operations Technology for Cold Regions,* Technical Area A, *Combat Operations Support,* Work Unit 002, *Excavation in Frozen Ground.*

Technical review of the manuscript was provided by Donald Garfield, Herbert Ueda, John Rand and Dr. Devinder Sodhi of CRREL.

The content of this report are not to be used for advertising or promotional purposes. Citation of brand names does not constitute an official endorsement or approval of the use of such commercial products.

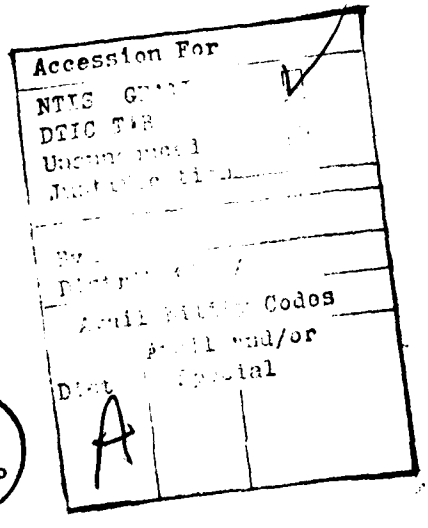

CONTENTS

ILLUSTRATIONS

FOREWORD

There are a multitude of tasks that involve the cutting, drilling, or excavating of natural ground materials and massive structural materials. The required technology varies with the properties of the materials and with the scale of operations, but a broad distinction can be made on the basis of the strength, cohesion, and ductility of the material that is to be worked. In weak materials that have little cohesion (e.g. typical soils) the forces and energy levels required for separation and disaggregation are often small compared with the forces and energy levels required for acceleration and transport, and materials handling technology dominates the consideration. By contrast, in strong materials that exhibit brittle fracture characteristics (e.g. rock, concrete, ice, frozen ground) the forces and energy levels required for cutting and breaking are high compared with those required for handling the broken material, and the technical emphasis is on cutting and breaking processes.

CRREL has long been concerned with excavating and drilling in ice and frozen ground, and over the past decade systematic research has been directed to this technical area. The research has covered a wide range of established technologies and novel concepts but, for short term applications, interest has necessarily centered on special developments of proven concepts. In particular, there has been considerable concern with direct mechanical cutting applied to excavation, cutting, and drilling of frozen soils, glacier ice, floating ice, and dense snow. During the course of this work, numerous analyses and design exercises have been undertaken, and an attempt is now being made to develop a systematic analytical scheme that can be used to facilitate future work on the mechanics of cutting and boring machines.

In the industrial sector, rock-cutting machines are usually designed by applying standard engineering methods in conjunction with experience gained during evolution of successive generations of machines. This is a very sound approach for gradual progressive development, but it may not be appropriate when there are requirements for rapid development involving radical departures from established performance characteristics, or for operations in unusual and unfamiliar materials. A distinct alternative is to design more or less from first principles by means of theoretical or experimental methods, but this alternative may not be practically feasible in its more extreme form.

There are numerous difficulties in attempting a strict scientific approach to the design of rock-cutting machines. The relevant theoretical rock mechanics is likely to involve controversial fracture theories and failure criteria, and to call for detailed material properties that are not normally available to a machine designer. Direct experiments are costly and time-consuming, and experimental data culled from the literature may be unsuitable for extrapolation, especially when (as is sometimes the case) they are described by relationships that violate the basic physics of the problem. Comprehensive mechanical analyses for rock-cutting machines have not yet

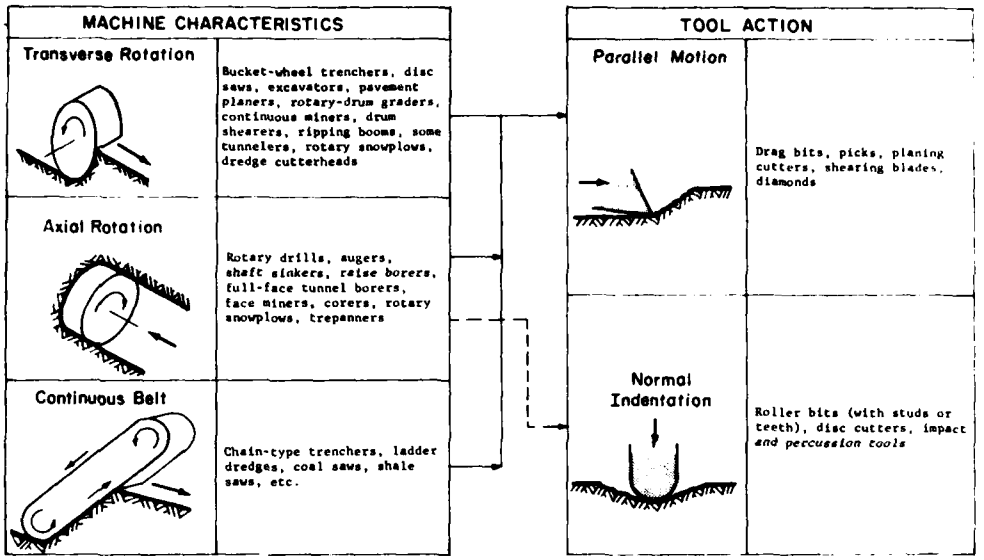

Classification of machines and cutting tools for analytical purposes.

evolved, and while established design principles for metal-cutting machine tools may be helpful, they do not cover all pertinent aspects. For example, there are usually enormous differences in forces and power levels between machine tools and excavating machines, and force components that can be almost ignored in a relatively rigid machine tool may be crucial design factors for large mobile rock cutters that are highly compliant.

In dealing with cold regions problems where neither outright empiricism nor highly speculative theory seem appropriate, some compromise approaches have been adopted. While simple and practical, these methods have proved useful for analysis and design of cutting and boring machines working under a wide range of conditions in diverse materials, and it seems possible that they might form the basis for a general analytical scheme. The overall strategy is to examine the kinematics, dynamics and energetics for both the cutting tool and the complete machine according to a certain classification, adhering as far as possible to strict mechanical principles, but holding to a minimum the requirements for detailed information on the properties of the material to be cut.

Kinematics deals with the inherent relationships defined by the geometry and motion of the machine and its cutting tools, without much reference to the properties of the material being cut. *Dynamics* deals with forces acting on the machine and its cutting tools, taking into account machine characteristics, operating procedures, wear effects, and material properties. *Energetics* deals largely with specific energy relationships that are determined from power considerations involving forces and velocities in various parts of the system, taking into account properties of the materials that are being cut.

These mechanical principles are applied in accordance with a classification based on the characteristic motions of the major machine element and the actual cutting

tools, as illustrated above. Machines are classified as *transverse rotation, axial rotation,* or *continuous belt,* while the action of cutting tools is divided into *parallel motion* and *normal indentation.*

Transverse rotation devices turn about an axis that is perpendicular to the direction of advance, as in circular saws. The category includes such things as bucket-wheel trenchers and excavators, pavement planers, rotary-drum graders, large disc saws for rock and concrete, certain types of tunneling machines, drum shearers, continuous miners, ripping booms, some rotary snowplows, some dredge cutterheads, and various special-purpose saws, millers and routers. *Axial rotation* devices turn about an axis that is parallel to the direction of advance, as in drills. The category includes such things as rotary drills, augers and shaft-sinking machines, raise borers, full-face tunnel boring machines, corers, trepanners, some face miners, and certain types of snowplows. *Continuous belt* machines represent a special form of transverse rotation device, in which the rotor has been changed to a linear element, as in a chain saw. The category includes "digger chain" trenchers, ladder dredges, coal saws, shale saws, and similar devices.

In tool action, *parallel motion* denotes an active stroke that is more or less parallel to the surface that is being advanced by the tool, i.e. a planing action. Tools working this way include drag bits for rotary drills and rock-cutting machines; picks for mining and tunneling machines; teeth for ditching and dredging buckets; trencher blades; shearing blades for rotary drills, surface planers, snowplows, etc.; diamond edges for drills and wheels; and other "abrasive" cutters. *Normal indentation* denotes an active stroke that is more or less normal to the surface that is being advanced, i.e. one which gives a pitting or cratering effect such as might be produced by a stone chisel driven perpendicular to the surface. Tools working this way include roller rock bits for drills, tunneling machines, raise borers, reamers, etc.; disc cutters for tunneling machines; and percussive bits for drills and impact breakers.

A few machines and operations do not fit neatly into this classification. For example, certain roadheaders and ripping booms used in mining sump-in by axial rotation and produce largely by transverse rotation, and there may be some question about the classification of tunnel reamers and tapered rock bits. However, the classification is very satisfactory for general mechanical analysis.

Complete treatment of the mechanics of cutting and boring is a lengthy task, and in order to expedite publication a series of reports dealing with various aspects of the problem have been printed in the order in which they were finished. This report completes the planned series, which consists of the following items:

1. Kinematics of transverse rotation machines (Special Report 226, May 1975)
2. Kinematics of axial rotation machines (CRREL Report 76-16, June 1976)
3. Kinematics of continuous belt machines (CRREL Report 76-17, June 1976)
4. Dynamics and energetics of parallel-motion tools (CRREL Report 77-7, April 1977)
5. Dynamics and energetics of indentation tools (CRREL Report 80-21, September 1980)
6. Dynamics and energetics of transverse rotation machines (CRREL Report 77-19, August 1977)
7. Dynamics and energetics of axial rotation machines (CRREL Report 81-26, December 1981)
8. Dynamics and energetics of continuous belt machines (CRREL Report 78-11, April 1978)

MECHANICS OF CUTTING AND BORING
Part 7: Dynamics and energetics of axial rotation machines

Malcolm Mellor

INTRODUCTION

This report deals with force, torque, energy and power in machines such as drills and boring devices, where the cutting head rotates about a central axis while penetrating parallel to that axis (Fig. 1). Unlike the other two classes of machines dealt with in this series (transverse rotation machines and continuous belt machines), the axial rotation machines can employ either parallel-motion cutting tools or indentation cutters. Geometry and motion for axial rotation machines are dealt with in Part 2 of this series (*Kinematics of axial rotation machines*), while the dynamic and energetic aspects of cutting tools are covered in Part 4 (*Dynamics and energetics of parallel motion tools*) and in Part 5 (*Dynamics and energetics of indentation tools*).

Starting from a consideration of the forces developed on individual cutting tools, or segments of cutters, the thrust and torque on a complete cutting head is assessed, and simple relationships between thrust and torque are derived. Similarly, the energy and power needed to drive the cutting head are estimated and related to tool characteristics.

Design characteristics of existing machines are compiled and analyzed to give indications of thrust, torque, power, effective tool forces, nominal thrust pressure, power density, and specific energy.

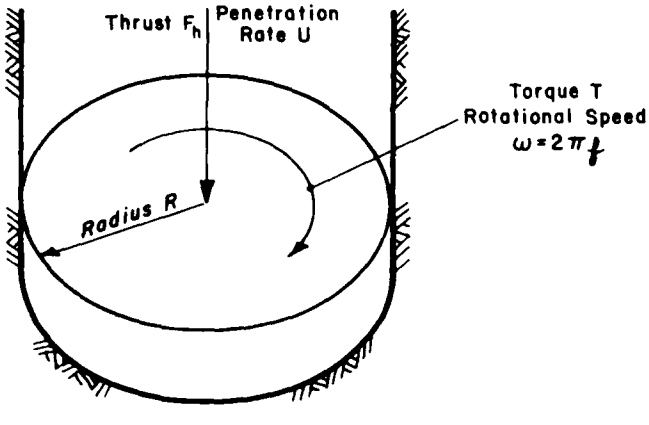

Figure 1. Axial rotation device.

TERMINOLOGY

Tool forces, or *cutter forces,* are the forces developed by the individual tools on a boring head. In the case of parallel-motion tools, the resultant force f for a single tool is usually resolved into orthogonal components f_n and f_t that are, respectively, normal and parallel to the work surface. Since the tool cuts along a helical path, f_n is not parallel to the machine's axis of penetration and rotation. In the case of roller cutters, the cutter force is usually taken to be the force on the axle of the roller cutter, although it is also possible to consider forces on the sections of the rim that are engaged in cutting. The axle force of a roller cutter is usually resolved into orthogonal components V and H that are, respectively, normal and parallel to the work surface. Since the axis of rotation of a roller cutter follows a helical penetration path, V is not exactly parallel to the machine's axis of penetration and rotation.

Head torque T is the net torque required to maintain the cutter operation at constant speed. An additional increment of torque is needed to overcome friction in the main head bearings, losses in gears or the transmission, fluid resistance (if the head is operating in liquid or mud) and, in the case of an auger, the conveying resistance of cuttings. In practical cases it may be difficult to separate the torque needed for cutting from the total torque.

Torque force F_t is a tangential force acting at the outer radius of the boring head R, such that $F_t = T/R$.

Torque power P_t is the power required to supply the net cutting torque T at a rotational speed of ω (angular velocity) or f (angular frequency or revolutions per unit time), i.e. $P_t = \omega T = 2\pi f T$. There is also a corresponding torque power needed to overcome losses and resistances other than direct cutting resistance.

Head thrust F_h is the force exerted parallel to the axis of rotation and penetration in order to provide force to the cutters in that direction. When F_h is a direct thrust against the boring head, reaction may be provided by deadweight, by deadweight and friction, by pressure-induced friction or shear against the hole wall, or by the wall, ceiling or floor of a chamber occupied by the boring machine. For deep vertical drilling in rock, the weight of the drill string can exceed the desired head thrust, and the string is then held in tension at the upper end. F_h is supplied by tension in raise borers, and in principle it can be supplied by tension when a short mandrel advances in a pilot hole ahead of the main borer.

Thrust power P_p is the power needed to supply the head thrust force F_h while advancing the boring head at an axial velocity U, i.e. $P_p = F_h U$.

Head power P_h is the power required to turn and thrust the boring head against the cutter resistance, i.e. $P_h = P_t + P_p$. In many cases $P_p \ll P_t$, so that $P_h \approx P_t$.

Machine power P_m is the total power of a drilling machine. It includes the head power P_h, the power needed to overcome losses at the boring head, power needed to convey cuttings, and power for other auxiliary systems.

Unit thrust force is the head thrust divided by the hole diameter, i.e. $F_h/2R$. It gives a measure of the cutter loading. In drilling technology it is sometimes referred to as "bit weight," although that term is more properly reserved for the total thrust.

Nominal head pressure is the head thrust per unit area, i.e. $F_h/\pi R^2$. It provides an index of thrust capability that can be used for comparing machines and applications.

Power density is the head power per unit area, i.e. $P_h/\pi R^2$ for a flat-face machine. If the machine cuts a conical or domed face, the quantity $P_h/\pi R^2$ can be referred to as nominal power density.

The *specific energy,* or *process specific energy,* E_s is the energy consumed per unit volume of penetration or, alternatively, the head power divided by the volumetric penetration rate, $P_h/\pi R^2 U$. An *overall specific energy* can be defined on the basis of total machine power P_m divided by the volumetric penetration rate $\pi R^2 U$.

A *dimensionless performance index* can be defined by dividing the process specific energy E_s by the uniaxial compressive strength of the material σ_c, assuming that both the cutting process and the strength test involve brittle fracture.

TOOL FORCES

An axial rotation device can use parallel motion tools, such as drag bits, blades, or abrasive grains. Alternatively, it can use rolling indentation tools, such as discs, studded rollers, or toothed rollers. The dynamics and energetics of the tools themselves are covered in Parts 4 and 5, and here the concern is with the relation of tool performance to the overall characteristics of the machine.

Parallel motion tools

Consider a coring or trepanning device (Fig. 2) which has a single cutter set with its cutting edge along a radial (i.e. the tool cuts orthogonally). The tool is narrow in relation to the radius from the center of rotation, so that there is no significant difference in velocity between the inside and outside edges of the tool. This tool behaves essentially the same as a cutter that travels in a straight line, and the cutting force, which can be resolved into orthogonal components f_n and f_t normal and parallel to the working surface respectively, is representable by the empirical equations:

$$f_n = k_n(\ell/\ell_r)^a \tag{1}$$

$$f_t = k_t(\ell/\ell_r)^b \tag{2}$$

where k_n and k_t are proportionality constants with dimensions of force (representing tool geometry and rock properties), ℓ is the tool's depth of penetration measured perpendicular to the work surface, ℓ_r is the tool tip radius (introduced for convenience to make ℓ dimensionless), and a and b

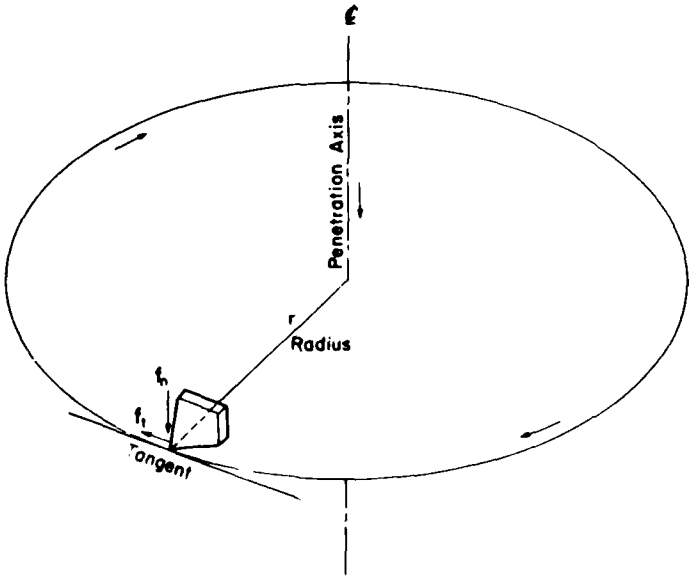

Figure 2. Narrow cutting tool planing orthogonally around a circular (or helical) track.

are fractional dimensionless exponents. Justification for this representation can be found in Part 4, and other applications are discussed in Parts 6 and 8.

Equations 1 and 2 are only approximate empirical relations, and for practical ranges of the cutting depth ℓ it may be satisfactory to replace them by linear equations of the form

$$f_n = A_n + k_n(\ell/\ell_r) \tag{3}$$

$$f_t = A_t + k_t(\ell/\ell_r) \tag{4}$$

where A_n and A_t are constants with dimensions of force, representing the force intercept for $\ell = 0$. It might be noted that in this linear form the normalizing parameter ℓ_r can be dispensed with by changing the dimensions of k_n and k_t. In some circumstances, e.g. narrow tools or tools cutting deeply in soft material, the constants A_n and A_t are small, and it is sufficient to assume direct proportionality:

$$f_n = k_n(\ell/\ell_r) \tag{5}$$

$$f_t = k_t(\ell/\ell_r) \tag{6}$$

in which explicit reference to ℓ_r can be dispensed with.

Instead of a coring device with a single cutter, consider now a cutting head that has individual tools set at different radii r from the center of rotation. As long as there is sufficient radial spacing between the tracks of individual cutters, the tools on the outer portions of the cutting head will behave in much the same way as the single tool that was just discussed, but each tool will behave differently than its neighbors because it lies at a different radius r. As the head rotates and penetrates at constant speed, each point on the head follows a helical path, with the helices getting steeper as the radius r decreases. Thus the tool speed relative to the rock varies with r, and the tool penetration normal to the work surface also varies with r, as explained in Part 2. For tools set very close to the center of the boring head, the complications are compounded by the fact the inside and outside edges of each tool travel at different speeds down helical paths of significantly different inclination. At the center of rotation itself, the helical penetration path becomes infinitely steep, and the behavior of a tool there bears little relation to the behavior of a tool planing orthogonally along a flat surface.

In practical equipment, the "center-of-hole problem" can be dealt with by: a) drilling a small-diameter pilot hole, b) leaving a central core uncut and allowing it to break off periodically, c) using a pilot bit, or mandrel, that has scaled-down cutters or special geometry (such as a "spear-point"). Thus the dynamics of the remaining tools can be treated without worrying unduly about complications and inefficiencies as $r \to 0$. As far as torque and thrust on the boring head are concerned, cutters near the center of the head do not account for much of the totals, *provided that the center-of-hole problem is being dealt with effectively.*

To simplify discussion and gain insight into the relationship between tool forces and total machine forces, some idealization of the problem is called for. First of all, it is useful to assume that the cutting tools are arranged so as to completely cover the radius, with no overlap of adjacent kerfs, but with repetition of coverage in one revolution a possibility, and circumferential staggering of individual tools permissible (Fig. 3). This allows tool force to be expressed as force per unit width, f', with f' a continuous function of the radius r so as to permit integration with respect to r. Another assumption is that tool force is insensitive to variations in tool speed over the range that applies for cutters at significant distances from the center of rotation (this is not unreasonable according to data given in Part 4). Under these assumptions the tool force varies with the radius r only to the extent that the tool penetration normal to the advancing surface (ℓ) is itself a function of r.

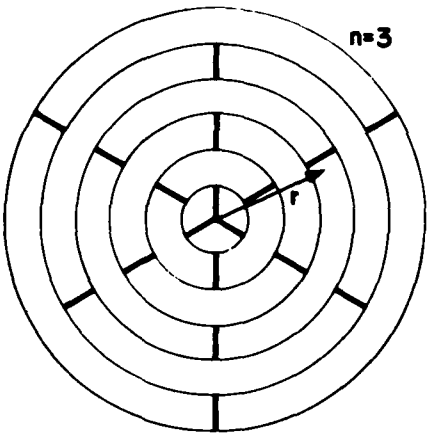

Figure 3. Tools arranged in a staggered pattern so as to give complete coverage of the radius with three repetitions per revolution.

The effective tool force per unit width, f', can be expressed fairly generally in terms of its orthogonal components f'_t and f'_n as

$$f'_t = A\,\ell^a \tag{7}$$

$$f'_n = B\,\ell^b \tag{8}$$

where the factors A and B are independent of r and of suitable dimensions to accommodate the power dependence of ℓ. However, for present purposes the assumption will be made that $a = b = 1$, i.e.

$$f'_t = A\,\ell \tag{9}$$

$$f'_n = B\,\ell \tag{10}$$

in which A and B have the dimensions of stress. If the helix angle for the tool penetration path at any radius r is α (see Part 2), then

$$\ell = \ell_a \cos\alpha \tag{11}$$

where ℓ_a is the *axial* penetration, given by

$$\ell_a = U/fn \tag{12}$$

in which U is the axial penetration rate, f is the number of revolutions per unit time, and n is the number of repetitions of kerf coverage in one revolution (or the number of tracking cutters). For a simple flat-end boring head, resolution of the cutter forces in the axial direction for a unit width at radius r gives

$$f'_t \sin\alpha + f'_n \cos\alpha = \frac{U}{fn}\left[A \sin\alpha \cos\alpha + B \cos^2\alpha\right]. \tag{13}$$

Resolution in a plane normal to the rotation axis, and in a direction tangential to the circle of rotation, gives

$$f_t' \cos\alpha - f_n' \sin\alpha = \frac{U}{fn}[A \cos^2\alpha - B \sin\alpha \cos\alpha]. \tag{14}$$

The angle α is

$$\alpha = \tan^{-1}\left(\frac{U}{2\pi rf}\right) \tag{15}$$

so that

$$\sin\alpha = \left[1 + \left(\frac{2\pi rf}{U}\right)^2\right]^{-1/2} \tag{16}$$

$$\cos\alpha = \left[1 + \left(\frac{U}{2\pi rf}\right)^2\right]^{-1/2} \tag{17}$$

and therefore

$$\sin\alpha \cos\alpha = \frac{(U/2\pi rf)}{1 + (U/2\pi rf)^2} \tag{18}$$

$$\cos^2\alpha = \frac{1}{1 + (U/2\pi rf)^2}\ . \tag{19}$$

The total axial thrust F_h can be taken as the sum of the tool force components in the axial direction, which in the idealized case is n times the integral of f' with respect to r:

$$F_h = \frac{U}{f} \int_{R_1}^{R_2} \left| \frac{A(U/2\pi rf) + B}{1 + (U/2\pi rf)^2} \right| dr$$

$$= \frac{1}{2\pi}\left(\frac{U}{f}\right)^2 \left[\frac{A}{2} \ln\left(1 + \left(\frac{2\pi rf}{U}\right)^2\right) + B\left(\frac{2\pi rf}{U}\right) - B \tan^{-1}\left(\frac{2\pi rf}{U}\right)\right]_{R_1}^{R_2}. \tag{20}$$

If the integration is taken between the center of rotation $r = 0$ and the outer edge of the boring head $r = R$, then

$$F_h = \frac{1}{2\pi}\left(\frac{U}{f}\right)^2 \left| \frac{A}{2} \ln\left(1 + \left(\frac{2\pi Rf}{U}\right)^2\right) + \frac{2B\pi Rf}{U} - B \tan^{-1}\left(\frac{2\pi Rf}{U}\right) \right|. \tag{21}$$

Since $2\pi Rf = u_t$, where u_t is the maximum tangential velocity in a plane normal to the axis of rotation:

$$F_h = \frac{1}{2\pi}\left(\frac{U}{f}\right)^2 \left| \frac{A}{2} \ln\left(1 + \left(\frac{u_t}{U}\right)^2\right) + B\frac{u_t}{U} - B \tan^{-1}\left(\frac{u_t}{U}\right) \right| \tag{22a}$$

$$= \frac{1}{2\pi}\left(\frac{U}{f}\right)^2 \left| \frac{A}{2} \ln\left(1 + \left(\frac{u_t}{U}\right)^2\right) + B\frac{u_t}{U} + B \tan^{-1}\left(\frac{U}{u_t}\right) - B\frac{\pi}{2} \right|. \tag{22b}$$

In Part 2, Figures 9 and 10 give representative values for u_t, and if these are combined with plausible values for U it is found that U/u_t is typically of order 10^{-2} or less. This being so, the last two terms of eq 22b combine to give a value that is an order of magnitude smaller than the second term. Furthermore, since B/A $(= f_n'/f_t')$ is typically of order unity (see Part 4), the first term of eq 22 can be neglected for many practical purposes, since its value may be less than 5% of the value of the second term. Making these simplifications, eq 22 reduces to

$$F_h \approx \frac{B}{2\pi}\left(\frac{U}{f}\right)^2 \cdot \frac{u_t}{U} \approx \frac{B}{2\pi}\left(\frac{U}{f}\right)^2 \cdot \frac{2\pi R f}{U}$$

i.e.

$$F_h \approx \frac{BUR}{f}. \tag{23}$$

B is a constant defined by:

$$B = \frac{f_n''}{\ell} = \frac{f_n'}{\ell_a \cos\alpha} = \left(\frac{fn}{U}\right)\frac{f_n'}{\cos\alpha}. \tag{24}$$

If we now define a mean effective cutting force $\bar{f}_n'$, such that

$$\bar{f}_n' = f_n'/\cos\alpha = \text{constant} \tag{25}$$

then

$$F_h \approx \left(\frac{fn}{U}\right)\bar{f}_n' \frac{UR}{f} = nR\bar{f}_n'. \tag{26}$$

This is a very complicated way of showing that, for machines such as rock augers, on which the tools follow very shallow helical penetration paths, the normal tool force and the axial component of tool force are approximately equal, and thus the thrust F_h is approximately equal to the sum of the normal tool forces. However, the derivation provides some insight into the effects of operating variables. For example, eq 23 indicates that the required thrust is proportional to the penetration speed, and inversely proportional to the rotational speed, although there is an implicit limitation because U/f has to stay within the range that gives efficient values of the tool chipping depth ℓ.

The torque T on the boring head is given by the summation of the moments developed by the individual tools. In a plane that is normal to the axis of rotation, the elementary tangential tool force at radius r is given by eq 14, and so the elementary moment, or torque, is that expression multiplied by the lever arm r. For the idealized case where unit cutting force f' is a continuous function of r, the total torque T is given by the integral of the elementary torque with respect to r. If there are n repetitions of tracking cutters, the integral has to be multiplied by n to get the total torque.

$$T = \frac{U}{f}\int_{R_1}^{R_2} r\left[\frac{A - B(U/2\pi rf)}{1+(U/2\pi rf)^2}\right]dr$$

$$= \frac{U}{f}\left(\frac{U}{2\pi f}\right)^2\left[\frac{A}{2}\left(\frac{2\pi rf}{U}\right)^2 - \frac{A}{2}\ln\left(1+\left(\frac{2\pi rf}{U}\right)^2\right) - B\left(\frac{2\pi rf}{U}\right) + B\tan^{-1}\left(\frac{2\pi rf}{U}\right)\right]_{R_1}^{R_2}. \tag{27}$$

If the integration is taken from the center of rotation $r = 0$ to the outer rim of the boring head $r = R$, then

$$T = \frac{U}{2f}\left[A\left\{R^2 - \left(\frac{U}{2\pi f}\right)^2 \ln\left(1+\left(\frac{2\pi Rf}{U}\right)^2\right)\right\} - \frac{BU}{\pi f}\left\{R - \frac{U}{2\pi f}\tan^{-1}\left(\frac{2\pi Rf}{U}\right)\right\}\right]. \tag{28}$$

Substituting $2\pi Rf = u_t$, eq 28 becomes

$$T = \frac{UR^2}{2f}\left[A\left\{1 - \left(\frac{U}{u_t}\right)^2 \ln\left(1+\left(\frac{u_t}{U}\right)^2\right)\right\} - \frac{2BU}{u_t}\left\{1 - \frac{U}{u_t}\tan^{-1}\left(\frac{u_t}{U}\right)\right\}\right]. \tag{29}$$

Noting again that U/u_t is likely to be of the order of 10^{-2} or less,

$$\left(\frac{U}{u_t}\right)^2 \ln\left(1+\left(\frac{u_t}{U}\right)^2\right) \sim 10^{-3} \qquad \text{(i.e. } << 1\text{)}$$

$$\frac{U}{u_t}\tan^{-1}\left(\frac{u_t}{U}\right) \sim 10^{-2} \cdot \frac{\pi}{2} \qquad \text{(also } << 1\text{)}.$$

Thus eq 29 can be approximated as

$$T \approx \frac{UR^2}{2f}\left[A - 2B\left(\frac{U}{u_t}\right)\right] \tag{30a}$$

or,

$$T \approx \frac{AUR^2}{2f}\left[1 - 2\frac{B}{A}\left(\frac{U}{u_t}\right)\right]. \tag{30b}$$

Since B/A $(= f_n'/f_t')$ is typically of order unity, the second term of eq 30b is likely to be much smaller than unity, so that eq 30b can be further simplified as

$$T \approx \frac{AUR^2}{2f}. \tag{31}$$

Referring back to eq 24 and 25, corresponding equations for f_t' can be written:

$$A = \frac{f_t'}{\ell} = \frac{f_t'}{\ell_a \cos\alpha} = \left(\frac{fn}{U}\right)\frac{f_t'}{\cos\alpha} \tag{32}$$

with the mean effective cutting force $\bar{f}_t'$ given by

$$\bar{f}_t' = \frac{f_t'}{\cos\alpha} = \text{constant}. \tag{33}$$

Substituting into eq 31, the approximate expression for the torque becomes

$$T \approx \left(\frac{fn}{U}\right)\bar{f}_t' \cdot \frac{UR^2}{2f} = \frac{nR^2}{2}\bar{f}_t'. \tag{34}$$

This again seems a roundabout way to arrive at a fairly obvious result, but the rather tortuous derivation is a useful exercise, in that it allows examination of the changes that occur when U/u_t is significantly greater than the typical 10^{-2} value.

The approximate expressions for thrust F_n and torque T can be interrelated by the ratio of the orthogonal components of the cutting force:

$$\frac{\bar{f}'_n}{\bar{f}'_t} = \frac{F_h R}{2T} \approx \frac{F_h}{2F_t} . \tag{35}$$

This is a very useful little equation. If the ratio of f_n/f_t is known for the relevant operating conditions, say from laboratory tests, then the ratio of thrust to torque that is needed for a balanced design can be estimated. Alternatively, if F_h and T are measured during a drilling operation, then an effective mean value of f_n/f_t can be estimated. If, in the absence of any data, it is assumed that $f_n/f_t \approx 1$ (see Part 4), then the expectation is that the torque force F_t (defined as $F_t = T/R$) will be about half the down thrust.

Indentation tools

Consider a flat-face boring head which has a single taper-edge disc cutter set at a large radius r from the center of the boring head (Fig. 4). The axle of the disc cutter lies along a radial of the main boring head, and it is normal to the axis of rotation for the main boring head. The action of the disc cutter is essentially the same as the action for straight-line cutting on a plane surface, and therefore the orthogonal components of its axle force H and V are as given by eq 104 and 105 of Part 5:

$$H \approx \tfrac{1}{2} C_2 \ell^2 \sigma_c \tag{36}$$

$$V \approx \frac{2\sqrt{2}}{3} C_2 \ell^{3/2} R_c^{1/2} \sigma_c \tag{37}$$

where ℓ is the depth of penetration normal to the surface, R_c is the radius of the disc cutter, σ_c is the uniaxial compressive strength of the material, and C_2 is a dimensionless constant determined by the wedge angle of the rim of the disc and by the failure criterion of the material.

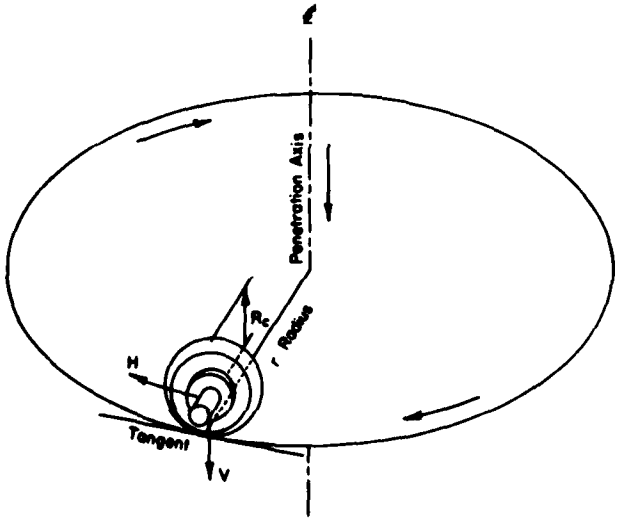

Figure 4. Disc cutter on a flat-face boring head.

In principle, the analysis that was outlined above for drag-bit tools could be repeated for disc cutters. However, the dependence of H and V upon ℓ is nonlinear in eq 36 and 37, and this complicates the required integrations. Because a typical borer of large diameter operates at small values of the ratio U/u_t, it is justifiable to introduce the consequent simplifications immediately, taking the total thrust F_h as the summation of the individual cutter forces V, and the total torque T as the summation of the individual cutter movements Hr.

On a rigid boring head, all the cutters must penetrate to the same depth, and thus if all the cutters are of the same design they will be loaded equally. If the cutters are arranged so as to give uniform coverage of the working face, an effective operating width Δr can be assigned to each cutter, and the axle force can be expressed in terms of a force per unit of radius ($H/\Delta r = H'$, $V/\Delta r = V'$). If there are n cutters set exactly at each radius r (n tracking cutters), the thrust F_h and torque T are

$$F_h = n \int_{R_1}^{R_2} V' dr = n \left[V'r \right]_{R_1}^{R_2} \tag{38}$$

$$T = n \int_{R_1}^{R_2} H' r \, dr = \frac{n}{2} \left[Hr^2 \right]_{R_1}^{R_2}. \tag{39}$$

If the "center-of-hole" problem is dealt with adequately, R_1 can be taken as zero, and if R is the radius to the outer rim of the boring head

$$F_h \approx n V' R \tag{40}$$

$$T \approx (n/2) H' R^2. \tag{41}$$

If N is the number of cutters (or cutting tracks) needed to give single-pass coverage of the radius R, the effective width of a single cutter Δr is R/N, and therefore $V' = VN/R$ and $H' = HN/R$. Thus,

$$F_h \approx nNV \tag{42}$$

$$T \approx (n/2) NRH \tag{43}$$

and the ratio T/F_h is

$$\frac{T}{F_h} = \frac{R}{2} \cdot \frac{H}{V}. \tag{44}$$

From eq 36 and 37, a theoretical value of H/V is

$$\frac{H}{V} = \frac{3}{4} \left(\frac{\ell}{2R_c} \right)^{1/2} \tag{45}$$

and so

$$\frac{T}{F_h} = \frac{R}{2} \cdot \frac{3}{4} \left(\frac{\ell}{2R_c} \right)^{1/2} = \frac{3}{8\sqrt{2}} R \left(\frac{\ell}{R_c} \right)^{1/2}. \tag{46}$$

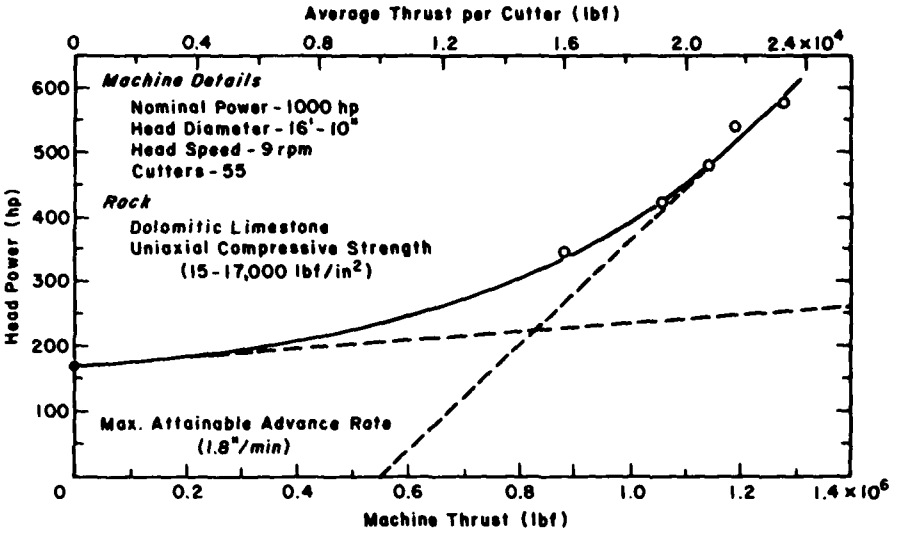

Figure 5. Measurements of head power as a function of axial thrust for a tunnel boring machine.

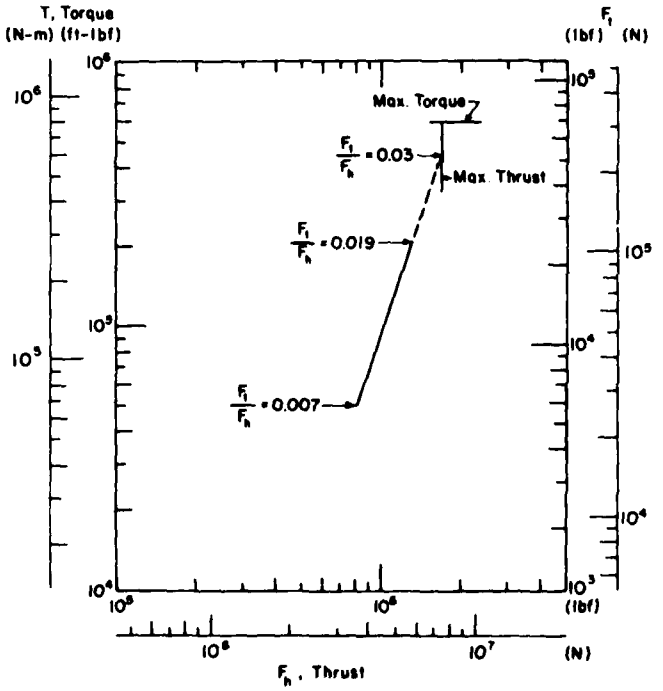

Figure 6. Torque and torque force as functions of axial thrust for a tunnel boring machine (using data from Figure 5).

If (ℓ/R_c) is of the order of 10^{-1}, then the torque force F_t (where $F_t = T/R$) ought to be an order of magnitude smaller than the thrust force F_h ($F_h/F_t = 12$ for $\ell/R_c = 0.1$). Another interesting implication of eq 46 is that an increase in the cutter penetration depth ℓ produces an increase in T/F_h or F_t/F_h.

Some experimental data tend to support eq 45 (Roxborough and Phillips 1975—see Part 5), while other data (Morrell and Larson 1974—see Part 5) fit better with the assumption that H/V is approximately proportional to ℓ. The same data indicate, respectively, that H is proportional to: a) V raised to a power slightly greater than unity, and b) approximately V^2. The magnitude of H/V in laboratory cutter experiments was found to be about 0.1 to 0.18 for weak rock by Roxborough and Phillips (1975), and from about 0.01 to 0.14 for hard rocks by Morrell and Larson (1974). If the last values are substituted into eq 44, the indication is that F_t/F_h is likely to be less than 0.09.

Figure 5 gives results of a lunch-break experiment with a tunnel boring machine in a Chicago sewer tunnel. With the cutters in contact with the face but with zero thrust on the machine, approximately 17% of the machine's total head power was needed to overcome friction of the boring head and its cutters. As thrust was gradually increased there was a corresponding gradual increase of power consumption, even though the cutters were not actually removing any rock. This reflects the effects of increasing frictional resistance in the bearings, and it is shown by a broken line in Figure 5 (dP/dF_h as $F_h \rightarrow 0$). Taking ordinates between this line and the power curve, net power is obtained as a function of thrust, and hence T and F_t can be obtained as functions of F_h (Fig. 6). According to these data, net working torque is almost exactly proportional to the third power of thrust, and apparent values of F_t/F_h are very low. At the upper limit of the data, $F_t/F_h = 0.019$, and at the extrapolation to the machine's maximum available thrust, $F_t/F_h = 0.03$. Corresponding values of the cutter penetration ℓ were not measured. There are too many uncertainties in this simple test to permit use of the data as a check on theoretical predictions. However, this numerical example serves to show how theory and experiment can be used to examine the design and performance of machines in a systematic way.

HEAD THRUST, THRUST PER UNIT WIDTH, AND NOMINAL HEAD PRESSURE

In an earlier section, simple theoretical relationships between tool forces and head thrust were derived. For simple cases of flat-face boring devices that penetrate slowly in relation to the rotational speed, the required head thrust was simply the sum of the tool force normal components. From this, it might be expected that boring machines would be designed to give a head thrust proportional to the diameter, assuming that the number of tracking cutters is not changed systematically with diameter. If the latter assumption does not hold, and the boring head is simply studded with cutters to fill up the available area (like a piece of sandpaper, or a diamond disc), then the head thrust would be more likely to be proportional to the square of the diameter, i.e. to the area.

At first glance it might seem that, since the chipping depth of a cutter increases with the normal force, it would be desirable to make the head thrust as high as possible. However, there are kinematic limits to useful penetration, and in very resistant material there are limits to the force that can be applied to a cutter.

In Figure 7 the maximum working thrust is plotted against head diameter for some existing machines, using logarithmic scales. Figure 7a gives data for augers and other mobile rotary rock drills, while Figure 7b gives data for full-face rotary tunnel boring machines. Oilfield rotary equipment is not represented in these plots, since the weight of pipe used in deep drilling typically exceeds the load limit of the bit, and tension has to be applied to keep the bit load to a safe level (see Fig. 8 for values).

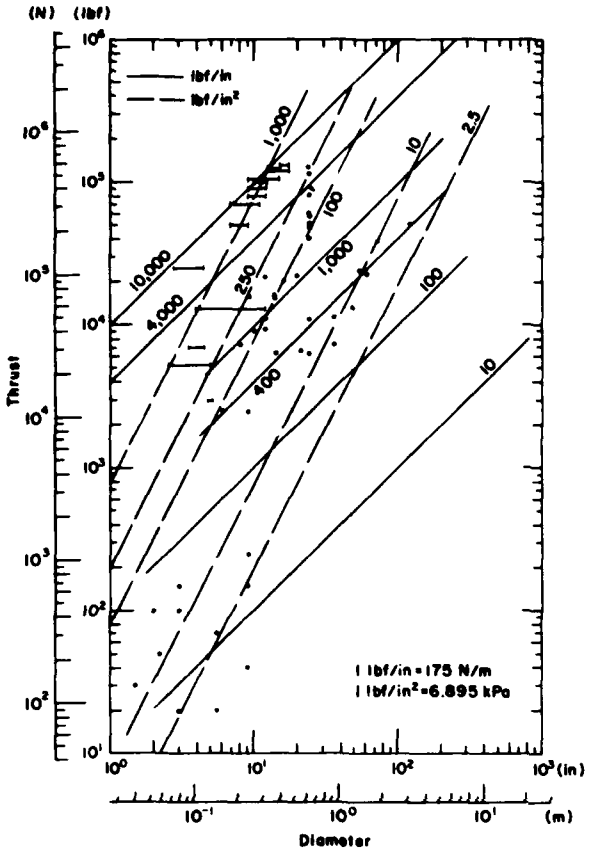

a. Augers and other mobile rotary rock drills.

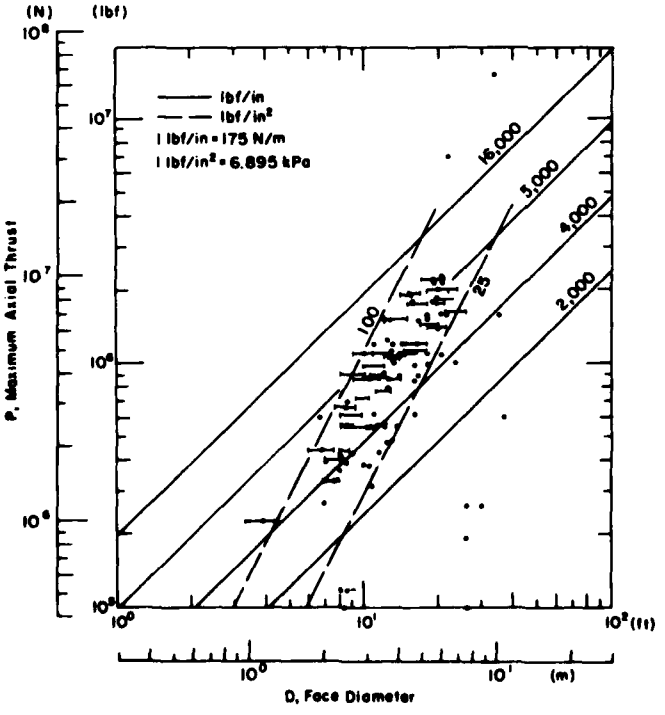

b. Full-face rotary tunnel boring machines.

Figure 7. Maximum working thrust plotted against head diameter for some existing machines. The lines indicate fixed levels of nominal head pressure and unit thrust force.

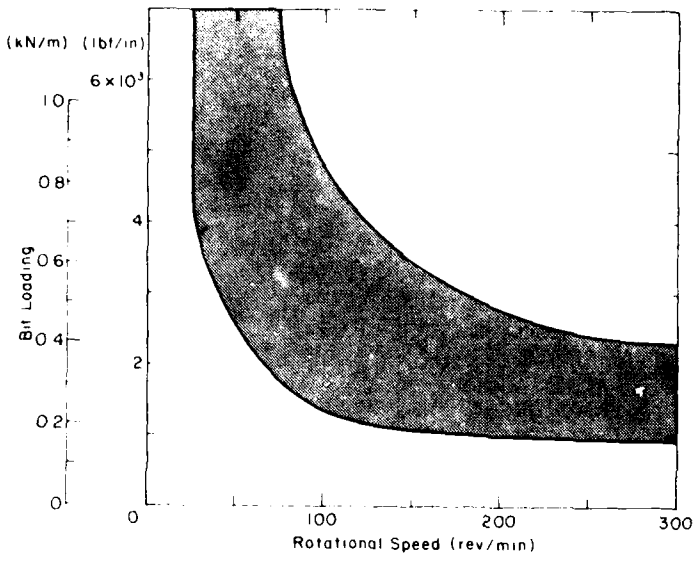

a. Bit loadings.

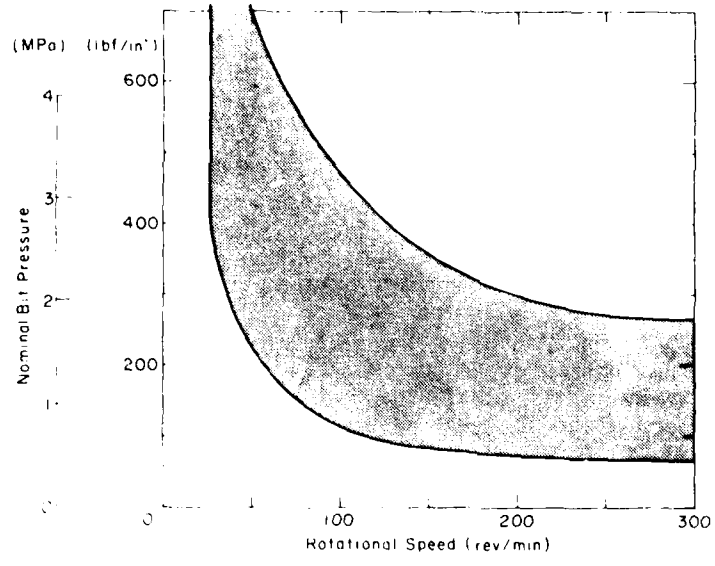

b. Nominal bit pressures.

Figure 8. Typical range of bit loadings and nominal bit pressures for roller rock bits, 6- to 12-in. diameter.

Simple theory, plus empirical knowledge that rotary rock bits should be loaded to a certain force per unit diameter, lead to an expectation that head thrust might be proportional to diameter. However, this is not borne out by the data for actual machines. There is understandably considerable scatter in the data, but the general trend is for the data bands to lie closer to a slope of 2 (i.e. $F_h \propto D^2$) than a slope of unity (i.e. $F_h \propto D$). In other words, the overall trend is for machines to develop a head thrust that is approximately proportional to the face area. In rotary rock drills, this

may result from the fact that the "strength" of a roller bit and its bearings is more or less proportional to the square of bit diameter.

Among the larger rock-cutting drills, the nominal head pressure ranges from about 10 lbf/in.^{2} to about 250 lbf/in.^{2} (0.07–1.7 MPa) for augers, and exceeds 1000 lbf/in.^{2} (7 MPa) for some rotary rock drills. The maximum unit thrust force (maximum head thrust divided by diameter) ranges from about 200 lbf/in. to about 8000 lbf/in. (35 kN/m–1.4 MN/m) for the same machines. For augers fitted with drag bits the unit thrust force can be associated with the normal tool force component f_n. Assuming that drag bits are arranged to give one complete coverage of the diameter (the equivalent of two radial cutting wings), the unit thrust force is approximately equal to f'_n. For standard rock cutting augers the range of values is 200 to 2000 lbf/in. (35–350 kN/m), which is not dissimilar to the values of f'_n measured in laboratory tests (see Part 4). Very powerful machines, such as roller-bit rotary rock drills and special augers developed for the Alaska Pipeline, extend the range of values up to about 8000 lbf/in. (1.4 MN/m), which is about the practical limit of loading for roller bits in the 6- to 10-in.-diameter (0.15–0.25 m) range.

Most of the data for hard-rock tunnel boring machines (Fig. 7b) fall quite neatly into a band that represents nominal head pressures from 25 to 100 lbf/in.^{2} (0.17–0.69 MPa). These values are smaller than corresponding values for drills, but when attention turns to unit thrust force the situation is reversed. Virtually all of the hard rock tunneling machines develop a maximum unit thrust in excess of 3000 lbf/in. (0.53 MN/m), with the larger machines giving up to about 12,000 lbf/in. (2.1 MN/m).

The maximum useful thrust for a hard rock tunnel boring machine (TBM) is limited by the capabilities of the bearings in the individual roller cutters. A typical roller cutter for a TBM is a frustum of a cone, with its surface carrying two to four disc cutters, or else an array of tungsten carbide studs. The disc type are arranged so that each disc has to deal with about 1 to 3 in. (25–75 mm) of radius on the face, while the studded type may have the studs staggered so as to dot the face with small craters spaced uniformly, perhaps at about 1-in. (25-mm) centers. The design working loads for single rollers are typically in the range 25,000 to 44,000 lbf (0.1–0.2 MN), but some machines are capable of applying average forces in excess of 60,000 lbf (0.27 MN) when the full head thrust is used.

POWER AND POWER DENSITY

The power needed to rotate a cutting head against the cutter resistance has already been considered in simple theoretical terms and, for cases where penetration is comparatively slow, related to the sum of tangential cutter forces.

In a real machine it is not always easy to decide how much power is being used variously to cut, to overcome bearing resistance, to cycle and convey cuttings, to overcome fluid resistance, and so on. With electric drive, and with some hydraulic drives, it is fairly easy to measure total power for turning the cutting head, total power for turning the head at the same speed with the cutters backed-off from the work, and hence the net power used for the cutting process. With mechanical drive from an internal combustion engine, not much can be done along this line unless special instrumentation is fitted. For comparing real machines, the simplest course is to make the best estimate of the power that can be supplied continuously to the boring head, recognizing that some will be lost in the transmission, and that the remainder has to be used in overcoming all the resistances to rotation.

Figure 9 gives plots of head power, or installed power, against head diameter for three classes of machines. Lines have been drawn on the logarithmic plots to represent various levels of nominal power density, i.e. power divided by the cross-section area of the hole. The data for tunnel boring machines (Fig. 9c) indicate that power is roughly proportional to face area, with power density mainly in the range 0.02 to 0.06 hp/in.^{2} (20–70 kW/m^2). For typical commercial augers (Fig. 9a)

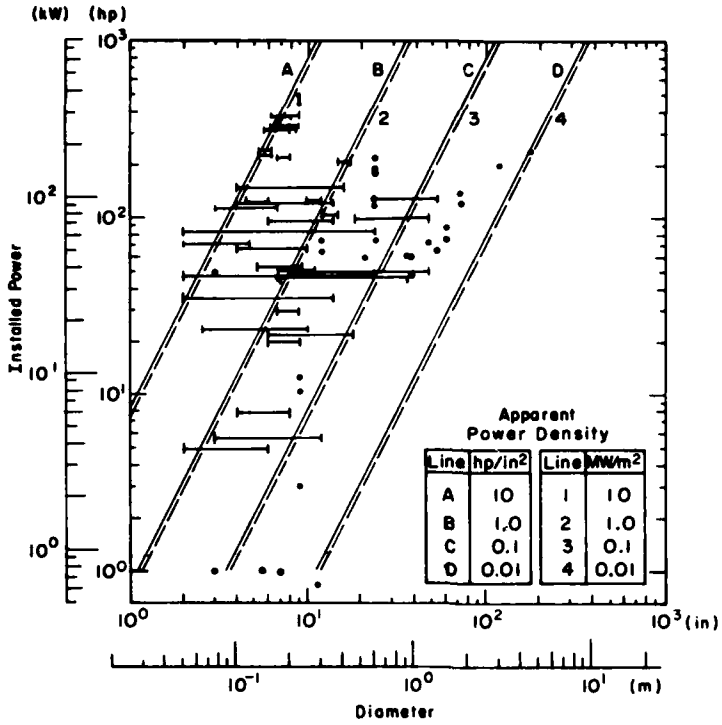

a. Augers.

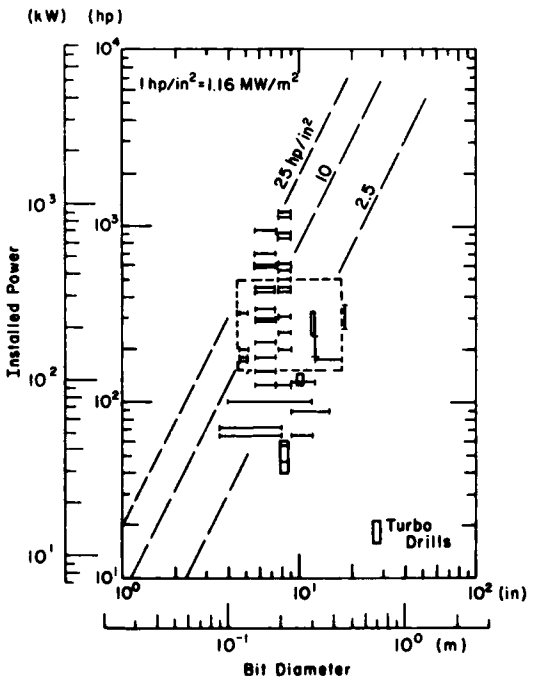

b. Rotary rock drills.

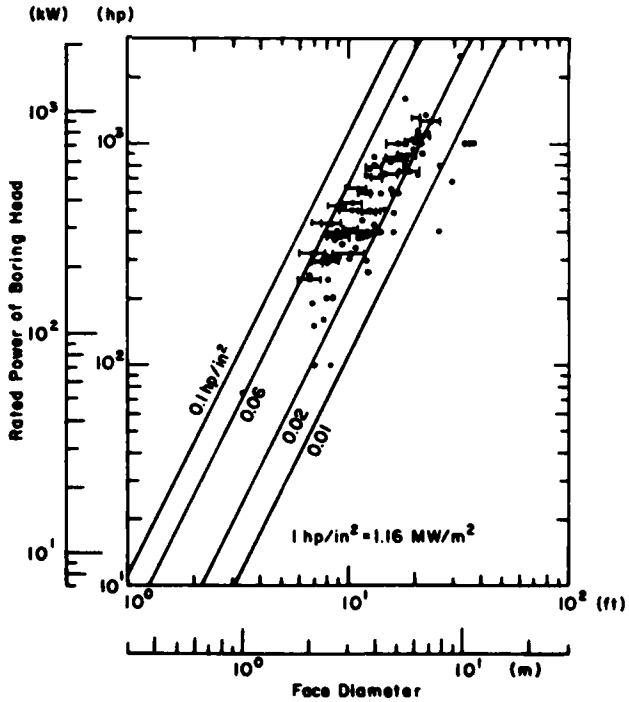

c. Tunnel boring machines.

Figure 9. Head power (or installed power) plotted against head diameter for some existing machines.

and for rotary rock drills, including oilfield rigs (Fig. 9b), there is not much correlation between power and hole size (or face diameter), since the installed power often serves the clearing and hoisting systems. Drills designed to handle bits of 4 to 12 in. (0.1–0.3 m) diameter can range in power from less than 10 hp (7.5 kW) to more than 1000 hp (750 kW). Thus the apparent power density for commercial rotary drilling equipment varies widely, from about 0.1 hp/in.^{2} (116 kW/m^2) to over 25 hp/in.^{2} (29 MW/m^2). These figures, which really are misleading, are much higher than the range of power densities for tunnel boring machines, and higher than the power densities of typical transverse rotation machines (see Part 6) or rock-cutting machines of the belt type (see Part 8).

The simple theory that was outlined earlier provides a clue to the variation of power density with face diameter. For both drag bits and roller cutters, the head torque is proportional to R^2 for constant chipping depth ℓ (eq 34 and 41):

$$T \approx k_1 R^2. \tag{47}$$

The rotational speed f has no explicit dependence on R, but there may be an implicit dependence resulting from the practice of holding the maximum tangential velocity u_t ($= 2\pi Rf$) within certain limits for a given type of cutting tool (see Fig. 9 and 10 of Part 2). If $2\pi Rf$ is assumed to be approximately constant (e.g. at 350 ft/min), then

$$2\pi f \approx k_2/R \tag{48}$$

and thus

$$P = 2\pi fT \approx k_3 R. \tag{49}$$

Finally, the power density is

$$\frac{P}{\pi R^2} = \frac{2\pi fT}{\pi R^2} \approx \frac{k_4}{R}. \tag{50}$$

In other words, power density is expected to be inversely proportional to the head radius (or diameter) according to these assumptions.

TORQUE

From the simple theoretical relations given in eq 34 and 41, the torque of a boring head ought to be approximately proportional to the square of the radius, or diameter, with the constant of proportionality determined largely by the mean tangential component of unit tool force $\bar{f}_t'$. If a variety of real boring machines are designed to develop tool forces of the same magnitude, then it might be expected that their torque capabilities would be proportional to the square of the head diameter, or bit diameter.

In Figure 10 the rated torque capability is plotted against rated diameter for rotary rock drills, augers, and hard-rock tunnel boring machines, using log-log scales. Lines with a slope of 2, indicating $T \propto D^2$, have been drawn to represent various values of force per unit width. For machines using drag bits, these force values represent $\bar{f}_t'$ when the bits give one complete coverage of the diameter (i.e. $n = 2$). For machines with roller cutters, the force values represent H' when the cutters are arranged to give one effective coverage of the diameter with $n = 2$.

The data for standard commercial augers and for tunnel boring machines show a reasonable correlation between torque and the square of diameter, since the points lie mostly within a band

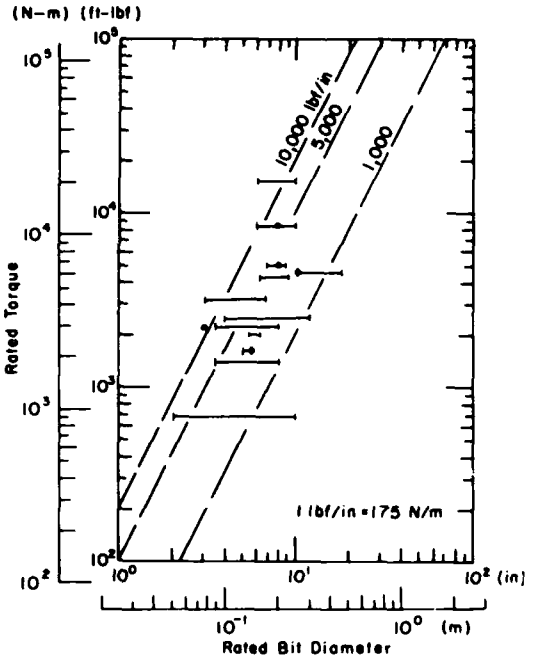

a. Rotary rock drills,

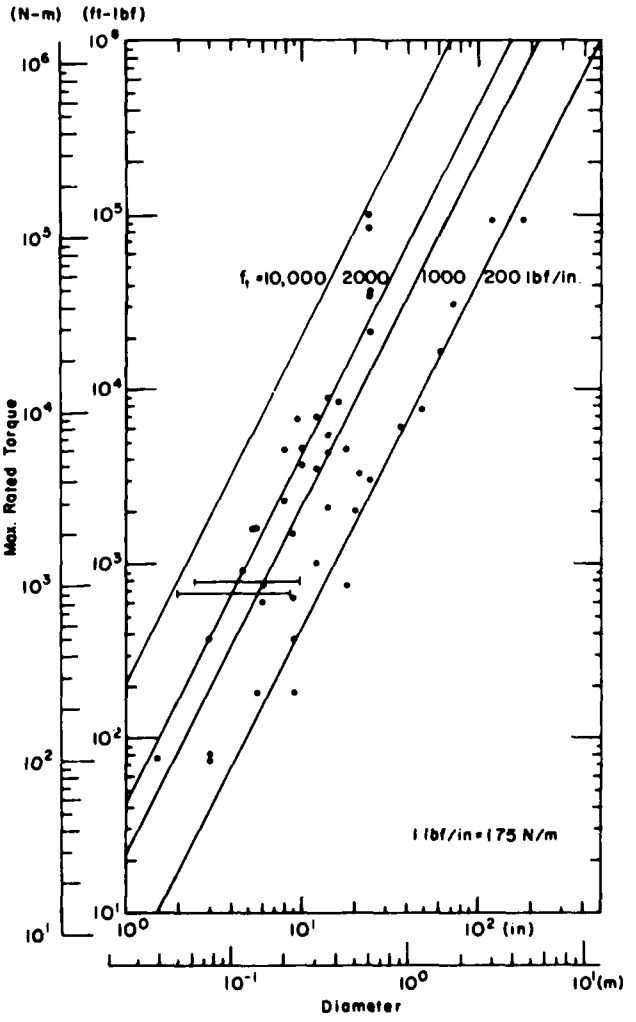

b. Augers.

Figure 10. Rated torque capability plotted against rated diameter for some existing machines.

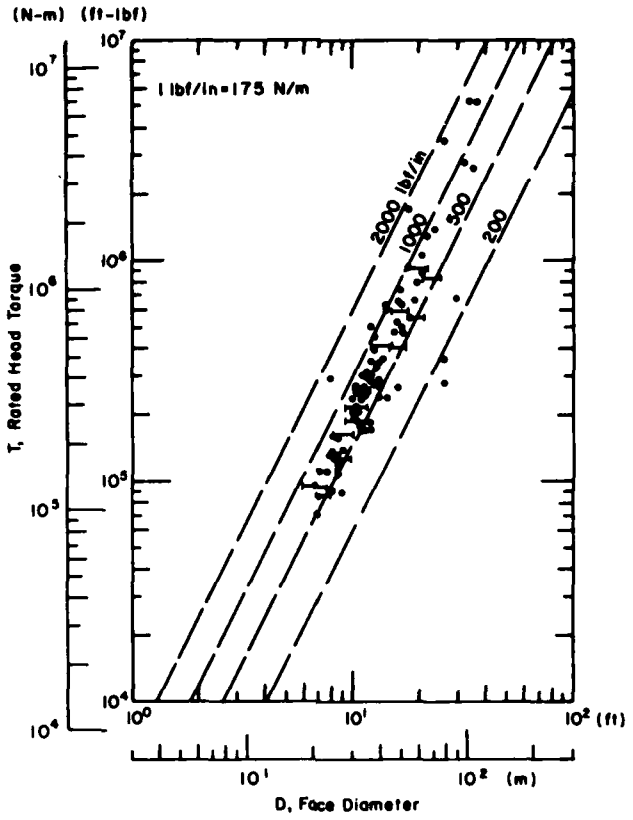

c. Hard rock TBM's.

Figure 10 (cont'd).

bracketed by 200 and 2000 lbf/in. (35-350 kN/m) as torque varies over 5 orders of magnitude. Rotary rock drills, and the special augers developed for construction of the Alaska Pipeline, have higher torque in relation to diameter than do the other machines.

In the discussion of power, it was pointed out that the actual power required for cutting is often difficult to separate out from the installed power, or the total rotary power. In the case of torque, it is not always clear what the rated torque of a machine really means. At what speed is the rated torque available? Is it continuously available? Is it the stall torque? Obviously the torque and the rotary power are proportional for a given head speed, so that the relationship between torque and diameter, and the relationship between rotary power and diameter, ought to be consistent with each other. If, from theoretical reasoning or from empirical evidence,

$$T = k_1 D^2 \tag{51}$$

then

$$P = 2\pi f T = 2\pi f k_1 D^2. \tag{52}$$

However, f usually varies systematically with D because the maximum tangential velocity $(u_t)_{max}$ tends to be kept within fairly narrow limits. Thus

$$f = \frac{(u_t)_{max}}{\pi D} \tag{53}$$

and

$$P = 2\pi f k_1 D^2$$

$$= 2k_1 (u_t)_{max} D \tag{54}$$

which is consistent with eq 49 in requiring proportionality between power and diameter. Taking values of k_1 = 125 lbf/in. (22 kN/m) and k_1 = 250 lbf/in. (44 kN/m) [which correspond respectively to the 500- and 1000-lbf/in. (88 and 175 kN/m) lines in Fig. 10], and assuming a value of $(u_t)_{max}$ = 350 ft/min (1.78 m/s), the corresponding values of power are $P = 2.65D$ hp and $P = 5.3D$ hp where D is in inches.

SPECIFIC ENERGY

The specific energy E_s is the work done to penetrate unit volume of material or, alternatively, the power consumption divided by the volumetric rate of penetration for the borer. If the energy input is strictly the energy needed to cut the material, E_s can be termed the *process specific energy*. On the other hand, if the estimate is based on total energy input to the boring head, or even to the complete machine system, E_s could be called the *overall specific energy*.

The power P used by the boring head is

$$P = 2\pi f T. \tag{55}$$

The volumetric penetration rate $\dot{v}$ is determined by the axial penetration rate U and the hole diameter D:

$$\dot{v} = (\pi/4) D^2 U. \tag{56}$$

Hence the specific energy E_s is

$$E_s = \frac{P}{\dot{v}} = \frac{8fT}{D^2 U}. \tag{57}$$

Specific energy can also be expressed in terms of the nominal power density of the boring head, $Q(= P/\pi R^2)$:

$$E_s = \frac{P}{\dot{v}} = \frac{Q}{U}. \tag{58}$$

This is a convenient relation for making rough estimates of potential penetration rate when Q is known and E_s can be guessed from experimental data or previous experience.

In Figure 11, power supplied to the boring head is plotted against the volumetric cutting rate for two classes of machines that are very different in size and operating characteristics. The upper group of data points is for hard rock tunnel boring machines, almost all of which are full-face rotaries using roller cutters of some kind. The power values are mostly derived from the installed power for head rotation, but some values have been checked by on-site observation. The cutting

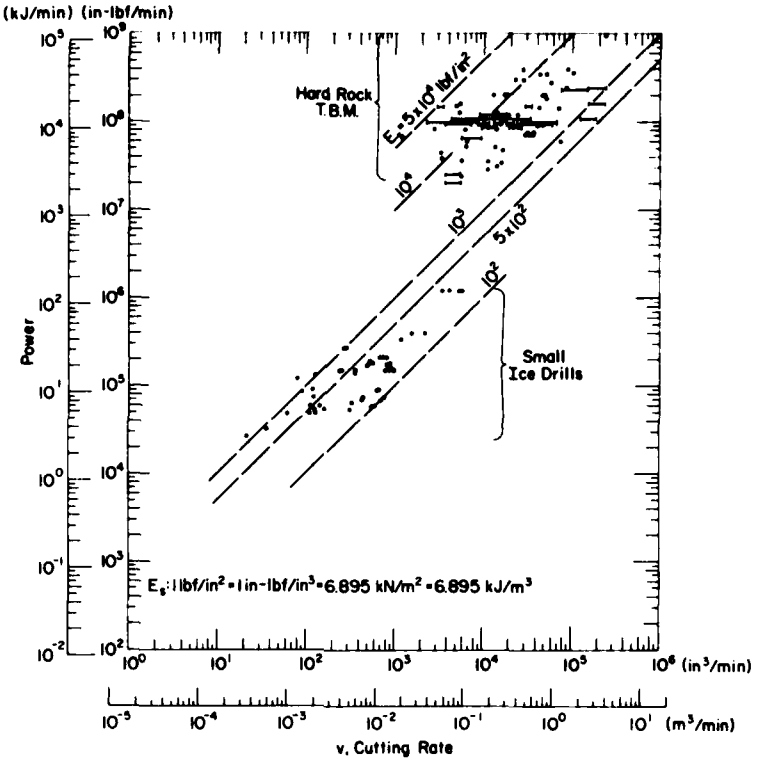

Figure 11. Power consumption at the boring head plotted against volumetric cutting rate for two classes of machines.

rates are good short-term rates, taken from project records or from direct observations by the author. Lines drawn through the data cluster, with a slope of unity on the log-log plot, represent various levels of specific energy. It might be noted again that specific energy has the same dimensions as a stress. The data should not be expected to necessarily show a close correlation between power and cutting rate, as the specific energy varies with machine characteristics, operating procedures, and material properties. The lower group of data points is for small drag-bit drills working in ice. Most of the power values are actual measured values of net power for cutting and clearing, while the cutting rates are short-term measured values (Kovacs et al. 1973). The range of specific energy for the ice drills is about one order of magnitude lower than the main range of values for rock tunneling machines.

Since the drills are at a *disadvantage* in terms of scale effect, the most obvious explanation of the difference in specific energy for the drills and the tunnel borers is that the drills are working in weaker material. This leads to discussion of the effect of material properties on performance.

EFFICIENCY AND PERFORMANCE INDEX

Other parts of this series have shown how specific energy can be correlated with the strength of the material that is being cut. For both indentation tools and drag tools, E_s ought to have a linear correlation with the uniaxial compressive strength σ_c in brittle material. However, it should not be expected that there will necessarily be a good correlation when data are taken for a wide range of machines and operating conditions, since the inherent efficiency of the machine and the effectiveness of the operating procedure are implicit variables.

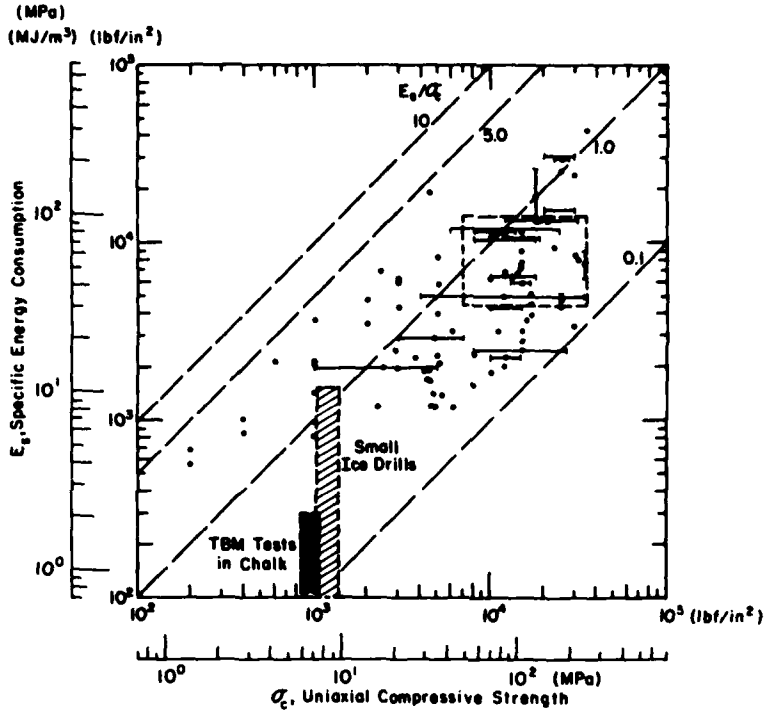

Figure 12. Specific energy plotted against uniaxial compressive strength for the two classes of machines represented in Figure 11.

Figure 12 gives data for tunnel boring machines and for small ice drills, E_s being plotted against σ_c on logarithmic scales. The diagonal lines drawn on the graph represent various values of E_s/σ_c, which is a dimensionless number that is taken here as an index of performance. Most of the data for tunneling machines lie within the range $0.2 < E_s/\sigma_c < 3$, which is more or less the same range as that defined by the experimental data for individual cutting tools of the indentation type (see Fig. 94 of Part 5). The data for small ice drills, which employ parallel-motion tools, lie somewhat lower than this band, say between 0.1 and 1.0. This agrees quite well with experimental results for individual drag bit tools (see Fig. 88 of Part 4), and with performance data for other types of machines that use parallel-motion tools (see Fig. 12 of Part 6 and Fig. 8 of Part 8).

The main utility of the performance index is in planning, preliminary design, and equipment appraisal. For machines that use indentation tools, it is overly optimistic at the present time to expect that E_s/σ_c can be less than 0.2, but $E_s/\sigma_c = 0.2$ is a realistic design goal. If performance data for a machine with indentation tools show $E_s/\sigma_c > 1.0$, then it is time to start worrying about the design of the machine itself, the selection and positioning of the cutters, or the way the equipment is being operated. For drag-bit machines, which seem to be somewhat more efficient in the relatively weak materials for which they are best-suited, the corresponding values of E_s/σ_c are slightly lower.

POWER REQUIREMENTS FOR CLEARANCE OF CUTTINGS

In tunnel boring with full-face rotary machines the power needed strictly for cutting can be very high, while the average power needed to convey cuttings away from the face may be very small. By contrast, in deep drilling the power needed purely for cutting may be almost negligibly small, while the power needed to remove cuttings is relatively very high. Thus, in design work and operational

planning, especially for new systems and novel applications, it is useful to assess the relative magnitudes of the power P_c needed for cutting and the power P_r needed for the removal of chips.

Because P_r has to be compared with P_c, an estimate of P_c is required. For some types of machines, the required estimate of P_c can be obtained directly from known characteristics, e.g. as summarized in Figure 11. With some other machines, such as rotary rigs for deep drilling, P_c has to be estimated indirectly, since the rotary power may be consumed largely in shearing the drilling fluid or by hole-wall friction. In such cases it may be sufficient to assume almost any reasonable value of specific energy E_s and multiply it by the penetration rate. For example, taking $E_s/\sigma_c \sim 1$ and assuming $\sigma_c \sim 10^4$ lbf/in.^{2} (70 MPa), $E_s \sim 10^4$ lbf/in.^{2} (70 MPa), then with an 8-in.-diameter (0.2-m) drill penetrating at $U \sim 1$ in./min (25 mm/min), $P_c \sim 1$ hp (0.75 kW). If the penetration rate U is an order of magnitude higher, say 1 ft/min (0.3 m/min), the rock is three times stronger, and E_s is very poor, say $E_s/\sigma_c \approx 2$, then $P_c \sim 100$ hp ($\sim$ 75 kW). This may seem a very wide range of uncertainty, but if $P_r \sim 1000$ hp ($\sim$ 750 kW), even the roughest estimate of P_c would suffice.

Minimum power requirements for lifting cuttings in a vertical hole

With a perfectly efficient system, the minimum amount of energy needed to lift unit volume of cuttings from depth h is simply the potential energy $\rho' gh$, where ρ' is the bulk density of the cuttings. In a continuous system the cuttings are removed at an average rate equal to the production rate of the boring head $\dot{v}$, so that the minimum power $(P_r)_{min}$ is

$$(P_r)_{min} = \dot{v}\rho gh = (\pi/4)D^2 U \rho gh \tag{59}$$

where ρ is the in-place density of the material that is being penetrated.

In order to relate this to the cutting power P_c, a ratio can be written in terms of energy as:

$$\frac{(P_r)_{min}}{P_c} = \frac{\dot{v}\rho gh}{E_s \dot{v}} = \frac{\rho gh}{E_s} . \tag{60}$$

E_s can vary from about 10^2 lbf/in.^{2} (0.7 MN/m^2) for ice and very weak rocks, to about 3×10^4 lbf/in.^{2} (200 MN/m^2) for hard rocks. The in-place density ρg can vary from less than 56 lbf/ft^3 (0.9 Mgf/m^3) to about 170 lbf/ft^3 (2.7 Mgf/m^3) for dense rock. The range of values for $\rho g/E_s$ might be from about 4×10^{-5} ft^{-1} (1.3×10^{-4} m^{-1}) in very strong material to about 4×10^{-3} ft^{-1} (1.3×10^{-2} m^{-1}) in very weak material. For $(P_r)_{min}$ to reach 10% of P_c, an efficient drill operating in very weak material only has to penetrate to about 25 ft (7.6 m). By contrast, a rather inefficient drill working in strong material would have to penetrate to about 2500 ft (760 m) before $(P_r)_{min}/P_c = 0.1$. The general point is that, while P_c is more or less independent of depth, $(P_r)_{min}$ increases linearly with depth.

All of this assumes that the lifting process is 100% efficient, but in reality it may be very inefficient. Introducing an efficiency factor η, such that the actual lifting power P_r is $(P_r)_{min}/\eta$, the relative power becomes

$$\frac{P_r}{P_c} = \frac{\rho gh}{\eta E_s} . \tag{61}$$

For some systems, e.g. continuous-flight augers working at shallow depth, η may be reasonably high. For other systems, e.g. air or gas circulation in very deep drilling, the overall efficiency may be so low as to make eq 61 almost meaningless.

Power consumption and efficiency in continuous-flight augers

In order to assess the energy consumed by an auger for vertical transport of cuttings, it is necessary to know something about the mechanics of the process. This seems to be a curiously neglected subject, but in Appendix A an attempt is made to develop some relevant theory.

The minimum energy needed to lift a mass of cuttings m through a vertical height h is mgh. The work W_a actually done by an auger working in the "centrifuge" mode is the work done against gravity, mgh, plus the work done against friction, $\mu_s F_n h/\sin\alpha$, where μ_s is the friction coefficient for cuttings on the flight, F_n is the normal force exerted against the flight by the mass m, and α is the effective mean helix angle of the flight.

$$W_a = mgh + \frac{\mu_s F_n h}{\sin\alpha} . \tag{62}$$

From eq A23,

$$F_n = mg\cos\alpha + \frac{\mu_w m}{\bar{R}} (\bar{u}_t - \bar{u}_s \cos\alpha)^2 \sin(\alpha+\beta). \tag{63}$$

The efficiency of the lifting process η is

$$\eta = \frac{mgh}{W_a} = \frac{mgh}{mgh + \mu_s F_n h/\sin\alpha}$$

$$= \frac{1}{1+\mu_s F_n/mg\sin\alpha} . \tag{64}$$

Estimates of η are best made by making numerical substitutions into the expression for F_n:

$$\frac{\mu_s F_n}{mg\sin\alpha} = \mu_s \cot\alpha + \frac{\mu_s \mu_w}{\bar{R}g\sin\alpha} (\bar{u}_t - \bar{u}_s\cos\alpha)^2 \sin(\alpha+\beta). \tag{65}$$

Since, from eq A25,

$$\bar{u}_s = \frac{\sin\beta}{\sin(\alpha+\beta)} \bar{u}_t \tag{66}$$

$$\frac{\mu_s F_n}{mg\sin\alpha} = \mu_s \left[\cot\alpha + \frac{\mu_w \bar{u}_t^2}{\bar{R}g\sin\alpha} \left(1 - \frac{\cos\alpha\sin\beta}{\sin(\alpha+\beta)}\right)^2 \sin(\alpha+\beta)\right]$$

$$= \mu_s \cot\alpha \left[1 + \frac{\mu_w \bar{u}_t^2}{\bar{R}g\cos\alpha} \left(\frac{\sin\alpha\cos\beta}{\sin(\alpha+\beta)}\right)^2 \sin(\alpha+\beta)\right]$$

$$= \mu_s \cot\alpha \left[1 + \frac{\mu_w \bar{u}_t^2}{\bar{R}g\cos\alpha} \frac{(\sin\alpha\cos\beta)^2}{\sin(\alpha+\beta)}\right] . \tag{67}$$

Following the numerical example given in Appendix A, and taking $\mu_s = \mu_w = \tan\alpha = \tan 30°$, values of β and $\bar{u}_t^2/\bar{R}g$ can be read from Figure A4. With $\bar{u}_t^2/\bar{R}g = 10$, $\beta = 16.7°$, and thus

$$\frac{\mu_s F_n}{mg \sin\alpha} = 1 + \frac{10 \times 0.3333 \times 0.5 \times 0.9174}{0.7278}$$

$$= 3.1.$$

For this case,

$$\eta = \frac{1}{1+3.1} = 0.244.$$

An efficiency of 24% might not sound very good, but it is much higher than the efficiency of a fluid circulation system is likely to be.

Since $\rho g/E_s$ for an auger might be in the range 4×10^{-5} to 4×10^{-3} ft^{-1} (1.3×10^{-4} to 1.3×10^{-2} m^{-1}), and h is likely to be in the range 10–100 ft (3–30 m) P_r is unlikely to exceed P_c when the auger flight is operating in the "centrifuge" mode.

When the auger flight is completely filled with cuttings it is hard to decide what the efficiency of the lifting process might be. However, it can certainly drop to very low levels, and when the auger is on the point of stalling because of high torque resistance from cuttings, P_r can obviously exceed P_c.

Air circulation

In air-circulation rock drilling, air has to be supplied at a rate sufficient to provide a flow velocity of about 3000 ft/min (15 m/s) for shallow depths. The required flow rate increases progressively with the depth of the hole, and to some extent with the drilling rate, but for present purposes it is

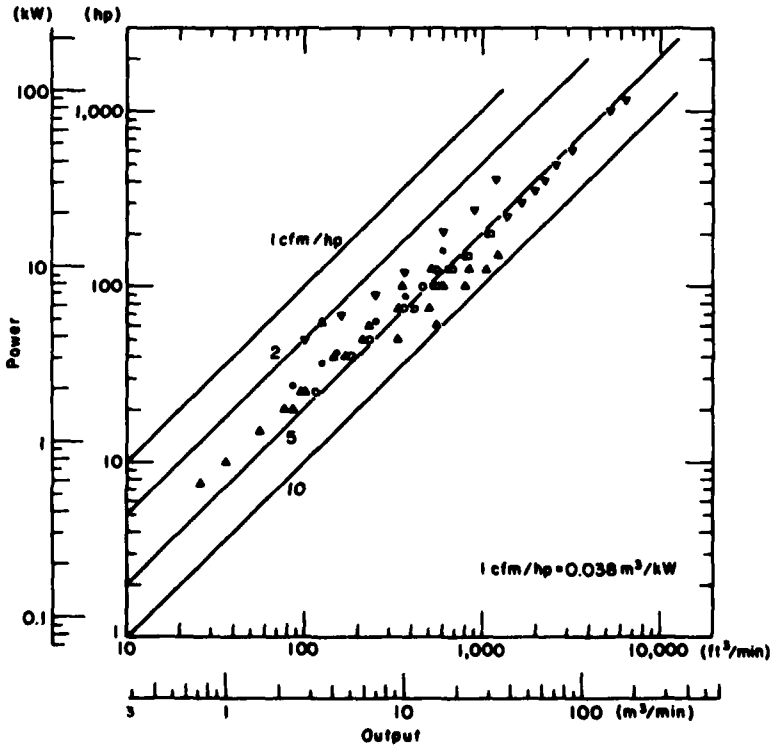

Figure 13. Power input plotted against volumetric air output for some existing air compressors.

unnecessary to go into these details, which are dealt with in handbooks of drilling technology (e.g. McCray and Cole 1973, International Association of Drilling Contractors 1974).

Flow rate requirements are given in terms of volume per unit time, but in order to estimate P_r and η these flow rate requirements have to be converted into power requirements. This can be done empirically by plotting flow rate against power for typical air compressors (Fig. 13). For a particular type of compressor with a given delivery pressure, there is a linear relation between flow rate and power, and for present purposes we can take the value 5 ft^3/min-hp (5 cfm/hp).

With a $7^7/_8$-in.-diameter bit and $4^1/_2$-in.-diameter drill pipe working at a depth of h = 1000 ft, the required air circulation rate might be about 750 ft^3/min for penetration at U = 1 ft/min, and about 720 ft^3/min for penetration at U = 0.05 ft/min. These requirements convert to P_r = 150 hp and P_r = 144 hp, respectively. The volumetric penetration rates are respectively $\dot{v}$ = 0.338 ft^3/min and $\dot{v}$ = 0.0169 ft^3/min, and the rock density ρ can be taken as 2.7 Mg/m^3, or 168 lb/ft^3. The efficiency of the lifting process η is

$$\eta = \frac{\dot{v}\rho g h}{P_r}. \tag{68}$$

Thus, with U = 1 ft/min, $\eta \approx 0.01$ (1%), and with U = 0.05 ft/min, $\eta \approx 6 \times 10^{-4}$ (0.06%).

Under these circumstances, the power P_r needed for removal of cuttings could easily be more than an order of magnitude greater than the power P_c needed for cutting.

Mud circulation

In oil-well drilling, cuttings are usually removed by circulation of special muds, with uphole velocity in the annulus typically in the range 65 to 200 ft/min (25 to 60 m/min), but sometimes greater. The required velocity varies inversely with the size of the hole, while the pump power depends on both flow velocity and input pressure. The required pressure is determined by the size of the annulus, the depth of hole, the circulation rate, and the density of the mud.

Using data from a suitable handbook of current practice (e.g. Institut Français du Pétrole 1980), estimates of the power P_r needed to remove cuttings can be made. Following the preceding example taken for air circulation, and assuming a $7^7/_8$-in.-diameter bit with $4^1/_2$-in.-diameter pipe and h = 1000 ft, circulation rates and power requirements can be obtained. Ignoring the small effect of drilling rate, and taking fairly high values for circulation, an annular velocity of about 60 m/min (200 ft/min) can be assumed, with a corresponding circulation rate of about 1200 L/min, or 320 gal./min. The pressure loss depends on the density of the mud, the hole, pipe and collar dimensions, and the flow rate. For mud with a specific gravity of 1.3, pressure loss might be about 20 $lbf/in.^2$ (1.4 bars) in the pipe bore, 50 $lbf/in.^2$ (3.5 bars) in the annulus between the pipe and the hole wall, maybe about 4 $lbf/in.^2$ (or about 0.3 bar) for the annulus around 30 ft (or 10 m) of $6^1/_4$-in.-diameter drill collar, and perhaps another 6 $lbf/in.^2$ (0.4 bar) inside the collar. This gives a total pressure loss (excluding losses in surface equipment) of 80 $lbf/in.^2$ (or 5.6 bars). Losses in surface equipment could be about 20% to 90% of this amount. Much bigger losses will occur in the bit nozzles, depending on how much pressure and hydraulic power is available from the pump. A modest nozzle loss for tricone or two-cone bits at 320 gal./min flow rate would be 400 $lbf/in.^2$ (28 bars). Thus the total pressure loss for this example is of the order of 500 $lbf/in.^2$ (35 bars) or more.

The corresponding hydraulic power is approaching 100 hp, and the required input power to drive the pump is about 110 hp (85% mechanical efficiency is usually assumed).

Taking calculated values of the cutting power P_c from the previous example on air circulation, the efficiency of the lifting process η is approximately 0.02 (2%) for penetration at 1 ft/min and 8×10^{-4} (0.08%) for penetration at 0.05 ft/min.

As was the case for air circulation, the power needed for lifting the cuttings is far greater than the cutting power under this set of circumstances.

LITERATURE CITED

Institut Français du Pétrole (1978) *Drilling Data Handbook.* Éditions Technip/Gulf Publishing Company (English edition published 1980), 413 p.

International Association of Drilling Contractors (1974) *Drilling Manual.* 9th edition.

Kovacs, A., M. Mellor and P.V. Sellmann (1973) Drilling experiments in ice. USA Cold Regions Research and Engineering Laboratory (CRREL) Technical Note, 25 p. (unpublished).

McCray, A.W. and F.W. Cole (1973) *Oil Well Drilling Technology.* University of Oklahoma Press, 492 p.

Mellor, M. and I. Hawkes (1972) Hard rock tunneling machine characteristics. *Rapid Excavation and Tunneling Conference, Chicago, 1972, Proceedings.* Chapter 66, p. 1149–1158.

Mellor, M. and I. Hawkes (1972) How to rate a hard-rock borer. *World Construction*, Sept, p. 21–23. (Also in *Ingenieria Internacional Construccion,* Oct 1972.)

Mellor, M. and P.V. Sellmann (1976) General considerations for drill system design. In *Ice-Core Drilling* (J.F. Splettstoesser, Ed.). University of Nebraska Press, p. 77–111. (Also CRREL Technical Report 164, 1975.)

Morrell, R.J. and D.A. Larson (1974) Tunnel boring technology: Disk cutter experiments in metamorphic and igneous rocks. U.S. Bureau of Mines, Report of Investigations 7961.

Roxborough, F.F. and H.R. Phillips (1975) The mechanical properties and cutting characteristics of the Bunter sandstone. Report by Department of Mining Engineering, University of Newcastle-upon-Tyne for Transport and Road Research Laboratory, Dept. of the Environment, United Kingdom.

Sellmann, P.V. and M. Mellor (1978) Large mobile drilling rigs used along the Alaska Pipeline. CRREL Special Report 78-4, 23 p.

APPENDIX A: VERTICAL CONVEYANCE BY CONTINUOUS-FLIGHT AUGERS

A continuous-flight auger conveys material vertically by sliding it up a helical ramp. Upward motion is resisted by the weight of the material, and by friction against the surface of the flight. In order for material to move up the flight, some reaction is required.

In principle there are three sources of reaction: 1) the bottom of the hole, 2) inertia when the rotation is accelerated, 3) friction against the wall of the hole. Inertial reaction from angular acceleration is not available when the auger is operated at constant speed, and reaction against the bottom of the hole cannot be invoked for deep drilling, as can be seen from the following argument.

Consider a layer of loose granular material lying on a long, smooth, uniform plane inclined at angle α to the horizontal (Fig. A1). Angle α is less than the angle of repose of the material, friction on the base is zero, and the layer (of uniform density ρ) is pushed up the slope by a barrier set perpendicular to the slope plane. The deadweight of the material against the wall is ($\rho g t L \sin\alpha$) per unit width, where L is the total length of the layer and t is its thickness. The maximum unit force R_{max} that the pusher can exert on the material before failure occurs is given by the passive pressure for plastic yielding, i.e.

$$R_{max} = \frac{1}{2}\left(\frac{1+\sin\phi}{1-\sin\phi}\right)\rho g t^2 \qquad \text{(A1)}$$

where ϕ is the friction angle of the granular material. Thus

$$\rho g t L \sin\alpha < \frac{1}{2}\left(\frac{1+\sin\phi}{1-\sin\phi}\right)\rho g t^2 . \qquad \text{(A2)}$$

Since $L \sin\alpha = H$, where H is vertical height

$$H < \frac{1}{2}\left(\frac{1+\sin\phi}{1-\sin\phi}\right) t \qquad \text{(A3)}$$

or with $\phi \approx 30°$,

$$H < 1.5t. \qquad \text{(A4)}$$

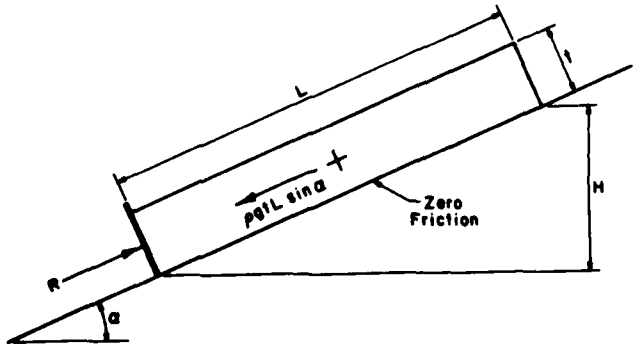

Figure A1. Granular material pushed up a smooth inclined plane.

This means that reaction against the bottom of the hole can only push material a short way. Consequently, for operation at constant speed, the only source of reaction is the hole wall.

To develop friction against the hole wall, there has to be a normal force, which in this case is a radial force. The three possible sources for such a force are: 1) lateral pressure from the weight of the material, 2) radial acceleration, or centrifugal force, 3) pressure developed when the scroll is jammed full of cuttings.

To estimate the lateral pressure developed by self-weight, consider again a uniform layer of granular material on an inclined plane, taking coordinate directions x, y, z respectively as parallel, transverse and normal to the slope plane. At depth z in the layer, the normal stress σ_z is $\rho g z \cos\alpha$ and the maximum lateral stress σ_y for the active stress state is

$$\sigma_y = \left(\frac{1-\sin\phi}{1+\sin\phi}\right)\sigma_z = \left(\frac{1-\sin\phi}{1+\sin\phi}\right)\rho g z \cos\alpha. \tag{A5}$$

If there is finite interfacial friction, with coefficients μ_s and μ_w for the scroll and the hole wall respectively, the frictional stresses on the scroll and the hole wall at depth z are, respectively,

$$\tau_{sF} = \mu_s \rho g z \cos\alpha \tag{A6}$$

$$\tau_{wF} = \mu_w \left(\frac{1-\sin\phi}{1+\sin\phi}\right)\rho g z \cos\alpha. \tag{A7}$$

There is also a frictional stress τ_{cF} against the cylindrical surface of the auger stem, which can be estimated by assuming a friction coefficient equal to that for the scroll:

$$\tau_{cF} = \mu_s \left(\frac{1-\sin\phi}{1+\sin\phi}\right)\rho g z \cos\alpha. \tag{A8}$$

We can now consider the static equilibrium of an inclined radial segment of the material which is just on the point of moving (Fig. A2). The general geometry of the helical surface is complicated (see Appendix B), and so for simplicity we treat the case where the width of the scroll is much less than the outside radius. Equating resistances to the driving friction:

$$\mu_w \left(\frac{1-\sin\phi}{1+\sin\phi}\right)\frac{\rho g t^2}{2}\cos\alpha_o \frac{(R_o\theta)}{\cos\alpha_o} < \mu_s \frac{\rho g t}{2}\cos\alpha_m \frac{(R_o^2-R_i^2)\theta}{\cos\alpha_m}$$

$$+ \mu_s \left(\frac{1-\sin\phi}{1+\sin\phi}\right)\frac{\rho g t^2}{2}\cos\alpha_i \frac{(R_i\theta)}{\cos\alpha_i} + \frac{\rho g t}{2}\frac{(R_o^2-R_i^2)\theta}{\cos\alpha_m}\sin\alpha_m \tag{A9}$$

where R_o and R_i are the radii of the hole and the auger stem respectively, θ is the angular size of the segment in horizontal projection, and t is the layer thickness. Thus

$$t\left(\frac{1-\sin\phi}{1+\sin\phi}\right)(\mu_w R_o - \mu_s R_i) \ll (R_o^2-R_i^2)(\mu_s+\tan\alpha_m) \tag{A10}$$

and if it is assumed that $\mu_w \approx \mu_s$:

$$\mu_s \left(\frac{1-\sin\phi}{1+\sin\phi}\right)t < (R_o+R_i)(\mu_s+\tan\alpha). \tag{A11}$$

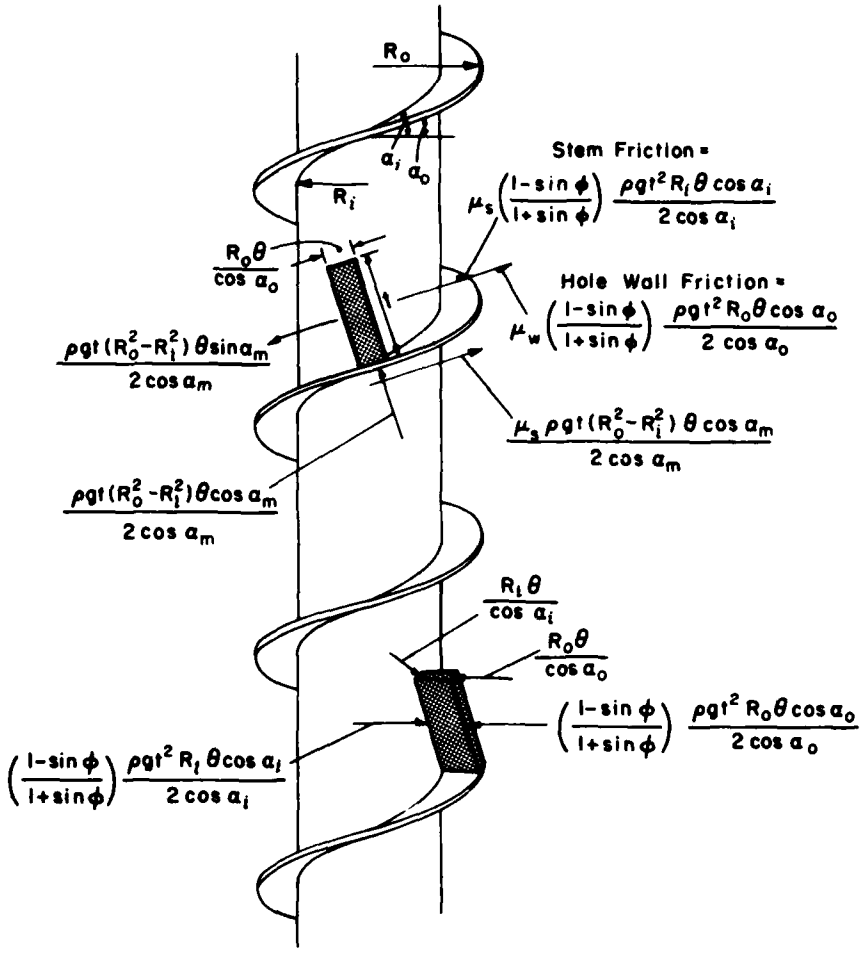

Figure A2. Equilibrium of an element of granular material on an auger flight, with only gravitational forces acting.

In order to initiate movement of material up the auger with only gravitational side pressure to provide wall friction:

$$\frac{t}{R_o + R_i} > \frac{\mu_s + \tan\alpha}{\mu_s} \left(\frac{1+\sin\phi}{1-\sin\phi}\right). \tag{A12}$$

Taking $30° \approx \phi \approx \alpha$, and $\mu_s \approx \mu_w \approx \tan 30°$

$$\frac{t}{R_o + R_i} > 6. \tag{A13}$$

But t is limited by the pitch of the auger P:

$$P = 2\pi R_o \tan\alpha \tag{A14}$$

$$t_{max} = P\cos\alpha = 2\pi R_o \sin\alpha. \tag{A15}$$

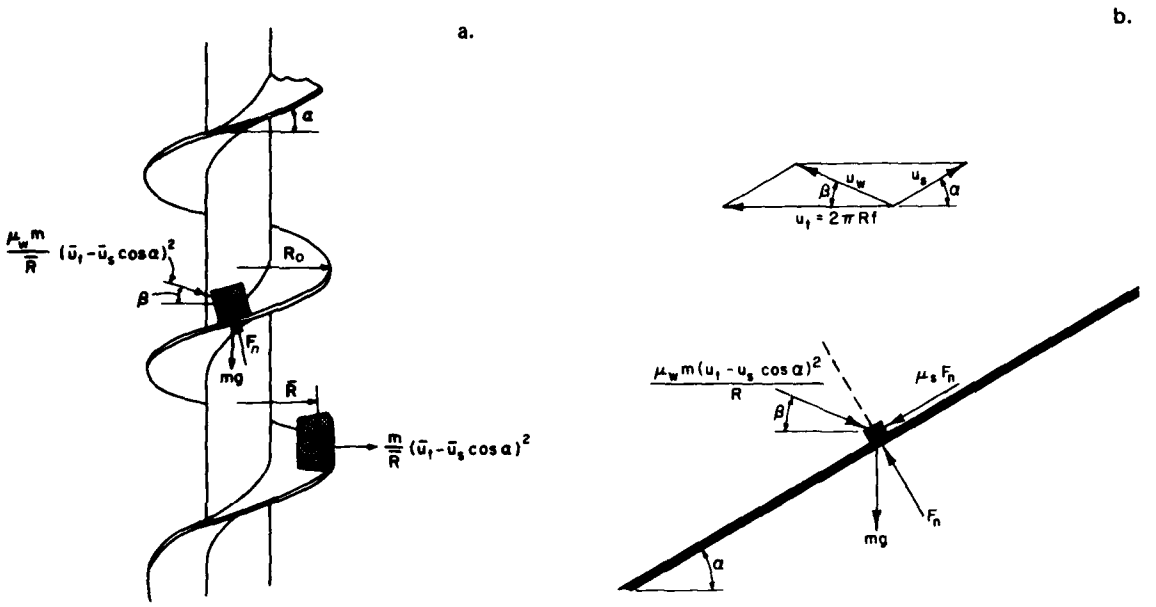

Figure A3. Forces acting on a block of material that is centrifuged against the hole wall by an auger flight.

With $\alpha = 30°$, condition A13 above implies that

$$6 < \frac{\pi}{1+(R_i/R_o)} \tag{A16}$$

which is impossible with R_i/R_o positive.

The general conclusion is that the lateral pressure developed by self-weight of granular material is unlikely to provide adequate reaction.

The only other source of hole wall reaction when the scroll is not jammed full of material is centrifugal force.

Consider a segment of material, or an isolated block, that lies on a flight where $\mu_s \geq \tan\alpha$ across the whole width of flight, $R_i < r < R_o$ (Fig. A3). The auger is rotating at constant speed, f rev/unit time, but the speed is not sufficient to carry material up the scroll. Neglecting friction against the auger stem, the forces resisting motion up the flight are $(mg \sin\alpha)$ and $(\mu_s\, mg\cos\alpha)$,where m is the mass of the segment. The segment rotates in a horizontal plane at f rev/unit time with its center of mass at radius $\bar{R}$ (Fig. A3). If there is a small clearance at the wall, the centrifugal force on the segment is resisted by friction on the scroll. Resolution in the radial direction gives

$$(2\pi f)^2 \bar{R} < \mu_s g \cos\alpha\,. \tag{A17}$$

If the rotational speed f is increased slowly, the material will slip on the scroll and move into contact with the wall when

$$f = \frac{1}{2\pi}\left(\frac{\mu_s g\cos\alpha}{\bar{R}}\right)^{1/2} \tag{A18}$$

in which $\bar{R}$ is a "mean effective radius." To check on the magnitude of the rotational speed needed to throw material against the wall, assume $\mu_s \approx \tan\alpha$ and $\alpha \approx 30°$. The required radial acceleration, $(2\pi f)^2 \bar{R}$, is then $\mu_s g\cos\alpha \approx g\sin\alpha \approx g/2$.

If the effective mean diameter ($2\bar{R}$) = 6 in., this means that 77 rpm is needed to throw cuttings into contact with the wall. Reference to Figure 9a on page 16 of Part 2 shows that this speed is below the range of f needed for effective operation of the auger bit. However, it can also be seen from eq A18 above that the required tangential velocity, $2\pi\bar{R}f$, has to increase in proportion to $\sqrt{\bar{R}}$, whereas for operation of drag bits $2\pi fR_o$ does not vary systematically with R_o. Taking a large value for mean effective diameter $2\bar{R}$, say 3 ft, the required value of f for contact with the wall is 31 rpm, and this is still within the range of speeds for effective bit operation.

Once the material has slid against the wall, the friction against the wall has to overcome the frictional resistance of the scroll and the weight of the material in order for sliding up the scroll to begin. The limiting equilibrium condition is given by resolution of forces parallel and normal to the surface of the scroll:

$$\mu_w m(2\pi f)^2 \bar{R} \cos\alpha = mg \sin\alpha + \mu_s F_n \tag{A19}$$

$$F_n = mg \cos\alpha + \mu_w m(2\pi f)^2 \bar{R} \sin\alpha \tag{A20}$$

and therefore the limiting radial acceleration is:

$$(2\pi f)^2 \bar{R} = g \frac{(\tan\alpha + \mu_s)}{\mu_w(1 - \mu_s \tan\alpha)}. \tag{A21}$$

If $\mu_w \approx \mu_s \approx \tan\alpha$ and $\alpha \approx 30°$, the radial acceleration needed to start the material sliding up the scroll is approximately 3 g. Referring back to the examples where mean effective diameters of 6 in. and 3 ft were taken, it is found that the corresponding minimum values of rotational speed for auger transport are, respectively, 187 rpm and 77 rpm. Both of these values of f are still within the normal operating range for drag bits. It should be pointed out, however, that there are no continuous flight augers as big as 3 ft in diameter.

Once the material begins to slide up the scroll, it no longer travels around the hole in a circular path, but instead follows a helical path up the wall. Taking the helix angle for the path up the wall as β, the material velocity relative to the wall as u_w, the velocity up the scroll as u_s, and the tangential velocity of the rotation as u_t ($= 2\pi R_o f$), the vector diagram for velocity is as shown in Figure A3b. The frictional reaction from the wall acts at angle β from the horizontal (Fig. A3), and resolution of forces for steady-state motion gives:

$$\frac{\mu_w m}{\bar{R}} (\bar{u}_t - \bar{u}_s \cos\alpha)^2 \cos(\alpha+\beta) = mg \sin\alpha + \mu_s F_n \tag{A22}$$

$$F_n = mg \cos\alpha + \frac{\mu_w m}{\bar{R}} (\bar{u}_t - \bar{u}_s \cos\alpha)^2 \sin(\alpha+\beta) \tag{A23}$$

with the bars denoting effective mean values for the center of mass of the material.

Eliminating F_n:

$$\frac{\mu_w}{\bar{R}} (\bar{u}_t - \bar{u}_s \cos\alpha)^2 [\cos(\alpha+\beta) - \mu_s \sin(\alpha+\beta)] = g(\sin\alpha + \mu_s \cos\alpha). \tag{A24}$$

From the velocity triangle,

$$u_s = \frac{\sin\beta}{\sin(\alpha+\beta)} u_t \tag{A25}$$

and therefore

$$\frac{\mu_w}{\bar{R}}\,\bar{u}_t^2\left(1-\frac{\cos\alpha\sin\beta}{\sin(\alpha+\beta)}\right)[\cos(\alpha+\beta)-\mu_s\sin(\alpha+\beta)] = g(\sin\alpha+\mu_s\cos\alpha). \tag{A26}$$

This can be rearranged as

$$\frac{\bar{u}_t^2}{\bar{R}g} = \frac{(1+\mu_s\cot\alpha)(1+\cot\alpha\tan\beta)}{\mu_w\cos\beta}\cdot\frac{\tan(\alpha+\beta)}{1-\mu_s\tan(\alpha+\beta)}. \tag{A27}$$

Equation A27 provides a solution for β, though not a neat analytical one. For purposes of illustration, we can assume

$$\mu_s \approx \mu_w \approx \tan\alpha \approx \tan 30^\circ$$

and give the solution for β in graphical form:

$$\frac{\bar{u}_t^2}{\bar{R}g} = (2\pi f)^2\frac{\bar{R}}{g} = \frac{2(1+1.7321\tan\beta)}{0.5774}\cdot\frac{\tan(30^\circ+\beta)}{1-0.5774\tan(30^\circ+\beta)}.$$

By substituting values of β and calculating $(\bar{u}_t^2/\bar{R}g)$, the relationship shown in Figure A4 is obtained. This indicates that, with the helix angle and friction coefficients assumed here, it would not be practically feasible to increase β above about 20°, and the maximum possible value of β would be about 30°.

The remaining question is how an auger functions when the flights are completely filled with material.

Suppose that an auger is turning slowly, and material is not centrifuged against the wall. The bit feeds cuttings onto the scroll, but they can only be pushed up a short distance. Cuttings then accumulate until they completely fill the flight, pressing against the hole wall, the auger stem, and the "floor and ceiling" of the scroll. This process can culminate in one of two ways: a) cuttings continue to feed into an immovable jam until limiting torque is reached (the turntable stalls or the stem

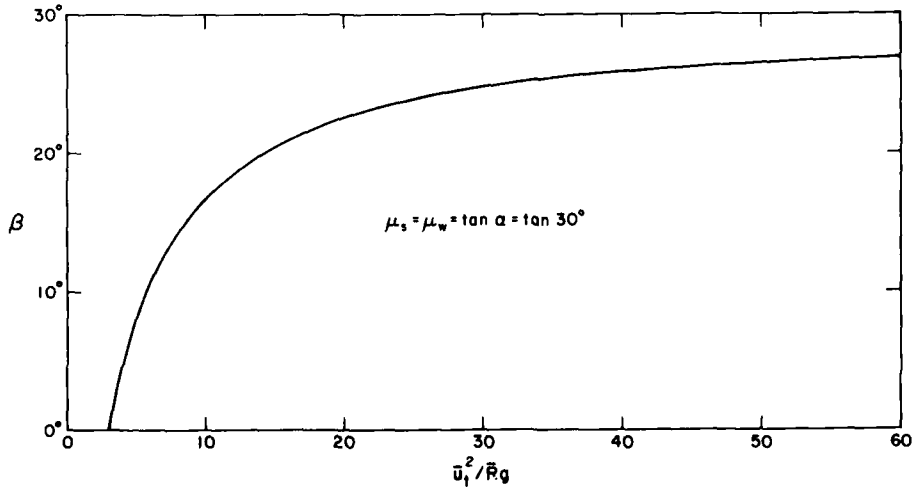

Figure A4. Solution of eq A27 for $\mu_s = \mu_w = \tan\alpha = \tan 30^\circ$.

fails in torsion), b) the cuttings are compacted up to the point where wall friction exceeds friction against the auger, and transport begins. The exact details of this process may be very complicated, but some useful insights can be gained by making simplifying assumptions.

Consider an auger bit feeding cuttings into a slowly rotating scroll until the flight is filled from top to bottom. Neglect the weight of the material, and assume that it develops an internal pressure p, which at any given section acts uniformly against the top and bottom of the flight, the stem of the auger, and the hole wall. Motion up the flight is resisted by friction against the flight and the stem, and a driving force for transport is provided by friction against the hole wall. For motion at constant speed we can equate the resistance to the driving force for a segment of material lying on a radial sector of the flight:

$$\mu_w p P R_o \theta > \mu_s p \frac{\theta}{\cos\alpha_m}(R_o^2 - R_i^2) + \mu_s p P R_i \theta \tag{A28a}$$

or

$$P(\mu_w R_o - \mu_s R_i) > \frac{\mu_s}{\cos\alpha_m}(R_o^2 - R_i^2). \tag{A28b}$$

If it is assumed that $\mu_w \approx \mu_s$ the condition for motion simplifies to

$$P\cos\alpha_m > R_o + R_i \tag{A29a}$$

or,

$$\sqrt{\left(\frac{2\pi R_m}{P}\right)^2 + 1} < \pi \tag{A29b}$$

where $R_m = \frac{1}{2}(R_o + R_i)$. Since $P\cos\alpha_m$ is the mean perpendicular distance t_m between adjacent wraps of the flight (neglecting flight thickness), and $(R_o + R_i)$ is the mean diameter D_m between center lines for the scroll, the simplified condition for motion with the flight jammed full is:

$$t_m > D_m. \tag{A30}$$

It is sometimes suggested that the helix angle of an auger ought to be small in order to assure good conveyance, but according to eq A30 a very small flight angle would cause the auger to jam if it runs full.

APPENDIX B: SURFACE AREAS ON A HELICAL FLIGHT AND ITS STEM

In considering the equilibrium of a radial segment of material on a flight, the area of the inclined scroll surface is needed, as is the contact area of the stem of the auger.

Take a radial segment that is defined by the projection of its base on a horizontal surface, where the center angle of the element is θ. At any radius there is an arc of length $r\theta$ on the horizontal surface, and a helical arc of length $s = r\theta \sec\alpha$ on the flight, where α is the helix angle at radius r. Thus

$$s = r\theta \sec\alpha \tag{B1}$$

and

$$\sec\alpha = \sqrt{1+(P/2\pi r)^2} \tag{B2}$$

where P is the pitch of the flight. The surface area of the flight over the segment (A_f) is

$$A_f = \int_{R_i}^{R_o} r\theta \sec\alpha \, dr \tag{B3}$$

where R_i and R_o are the radii of the stem and the outside of the scroll respectively. Because

$$r = (P/2\pi)\cot\alpha \tag{B4}$$

and

$$dr = -(P/2\pi)\operatorname{cosec}^2\alpha \tag{B5}$$

$$A_F = -\theta\left(\frac{P}{2\pi}\right)^2 \int_{\alpha_i}^{\alpha_o} \frac{d\alpha}{\sin^3\alpha}$$

$$= \frac{\theta}{2}\left(\frac{P}{2\pi}\right)^2 \left[\frac{1}{\sin\alpha\tan\alpha} + \ln\tan(\alpha/2)\right]_{\alpha_i}^{\alpha_o}. \tag{B6}$$

Substituting

$$(P/2\pi) = r\tan\alpha = R_i\tan\alpha_i = R_o\tan\alpha_o \tag{B7}$$

then

$$A_F = \frac{\theta}{2}\left[\frac{R_o^2}{\cos\alpha_o} - \frac{R_i^2}{\cos\alpha_i} + \ln\left(\frac{\tan(\alpha_o/2)}{\tan(\alpha_i/2)}\right)\right]. \tag{B8}$$

Substitutions for α can be made from

$$\cos\alpha = \frac{1}{\sqrt{1+(P/2\pi r)^2}} \tag{B9}$$

$$\tan(\alpha/2) = \pm\sqrt{\frac{1-\cos\alpha}{1+\cos\alpha}}. \tag{B10}$$

In the analysis of transport mechanisms, explanations are simplified and clarified by assuming that the flight is narrow relative to the total radius, i.e. $(1-R_i/R_o) \ll 1$. Under these circumstances, $\alpha_o \approx \alpha_i$ and

$$A_F \approx \frac{\theta}{2\cos\alpha_m}(R_o^2 - R_i^2) \tag{B11}$$

where α_m is a mean helix angle.

An inclined segment of material also has a contact with the stem of the auger, and this contact area tends to wrap itself around the stem. The length of the helical arc at radius R_i is

$$s = R_i\theta\sec\alpha_i\,. \tag{B12}$$

If the thickness of the segment measured normal to the helix is z, then the area of contact A_c is

$$A_c = sz = zR_i\theta\sec\alpha_i = z\theta R_i\sqrt{1+(P/2\pi R_i)^2}\,. \tag{B13}$$

If the flight is jammed full of material

$$z = P\cos\alpha_i \tag{B14}$$

and in this case

$$\begin{aligned} A_c &= sP\cos\alpha_i \\ &= P\cos\alpha_i R_i\theta\sec\alpha_i \\ &= PR_i\theta. \end{aligned} \tag{B15}$$

The same relationships apply to contact areas on the outside wall by substituting R_o and α_o for R_i and α_i.

A facsimile catalog card in Library of Congress MARC format is reproduced below.

Mellor, M.
Mechanics of cutting and boring. Part 7: Dynamics and energetics of axial rotation machines / by Malcolm Mellor. Hanover, N.H.: U.S. Cold Regions Research and Engineering Laboratory; Springfield, Va.: available from National Technical Information Service, 1981.
vi, 46 p., illus.; 28 cm. (CRREL Report 81-26.)
Prepared for Office of the Chief of Engineers by Corps of Engineers, U.S. Army Cold Regions Research and Engineering Laboratory under DA Project 4A762730AT42.
Bibliography: p. 27.
1. Cutting tools. 2. Drilling. 3. Drilling machines. 4. Drills. 5. Excavation. 6. Machines. 7. Mechanics. 8. Permafrost. 9. Rock drilling. I. United States. Army. Corps of Engineers. II. Army Cold Regions Research and Engineering Laboratory. III. Series: CRREL Report 81-26.

☆U.S. GOVERNMENT PRINTING OFFICE: 1982—500-992/369


FI
05